Journal of Power Sources 475 (2020) 228689

Contents lists available at ScienceDirect

Journal of Power Sources

journal homepage: www.elsevier.com/locate/jpowsour

Membranes for zinc-air batteries: Recent progress, challenges and perspectives

Misgina Tilahun Tsehaye [a], Fannie Alloin [a], Cristina Iojoiu [a,*], Ramato Ashu Tufa [b], David Aili [b], Peter Fischer [c], Svetlozar Velizarov [d]

[a] Univ. Grenoble Alpes, Univ. Savoie Mont Blanc, CNRS, Grenoble INP, LEPMI, 38 000, Grenoble, France
[b] Department of Energy Conversion and Storage, Technical University of Denmark, Building 310, 2800 Kgs, Lyngby, Denmark
[c] Applied Electrochemistry, Fraunhofer Institute for Chemical Technology ICT, Joseph-von-Fraunhofer, Straße 7, 76327, Pfinztal, Germany
[d] LAQV-REQUIMTE, Chemistry Dept., FCT, Universidade Nova de Lisboa, 2829-516, Caparica, Portugal

HIGHLIGHTS

- Performance determining properties of membranes for Zn-air batteries are presented.
- Seven types of membranes for Zn-air batteries are defined, discussed and compared.
- Strategies for minimizing zincate cross-over and Zn-dendrite growth are discussed.
- Research directions for developing membranes for Zn-air batteries are identified.

GRAPHICAL ABSTRACT

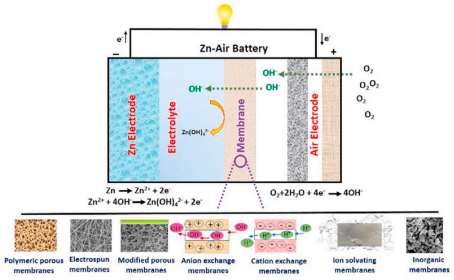

ARTICLE INFO

Keywords:
Zinc-air batteries
Porous membranes
Ion-exchange membrane
Electrospun nanofiber membranes
Zincate crossover
Zn-dendrites

ABSTRACT

Rechargeable Zinc (Zn)-air batteries are considered to be very attractive candidates for large-scale electricity storage due to their high volumetric energy density, high safety, economic feasibility and environmental friendliness. In Zn-air batteries, the membrane allows the transport of OH^- ions between the air electrode and the Zn electrode while providing a physical barrier between the two electrodes in order to prevent electrical short circuits. The performance of this battery is greatly affected by the physicochemical properties of the employed membrane. However, the development of appropriate membranes has received insufficient attention. In this paper, an overview of recent developments and a critical discussion of the state-of-the-art studies focusing on membranes for Zn-air batteries are provided. The membranes are classified in seven categories, which are discussed in light of their structure, properties and performances in Zn-air battery. Moreover, membrane synthesis and modification strategies to minimize the crossover of zincate ions and formation/growth of Zn-dendrites are presented. Finally, the remaining key challenges related to the membranes and the most promising future research directions are provided. The main objective of this work is to provide guidance for researchers and industries for the selection and development of appropriate membranes with the ultimate goal of commercializing rechargeable Zn-air batteries.

* Corresponding author.
E-mail address: cristina.iojoiu@lepmi.grenoble-inp.fr (C. Iojoiu).

https://doi.org/10.1016/j.jpowsour.2020.228689
Received 17 May 2020; Received in revised form 7 July 2020; Accepted 23 July 2020
Available online 18 August 2020

Table 1
Comparison of different metal-air batteries [43,44].

Battery systems	Li-air	Na-air	Mg-air	Al-air	Zn-air	K-air	Fe-air
Theoretical cell voltage (E^{o}_{cell}) (V)	2.96	2.27	3.09	2.71	1.65	2.48	1.28
Cost of metals (US $ kg^{-1})	20	2.5	2.3	1.9	2.6	1.0	0.5
Theoretical energy density (Wh kg^{-1})[a]	3458	1106	2840	2796	1087	935	763
Specific capacity (mAh g^{-1})	3861	1166	3833	2980	820	377	2974
Electrolyte for practical batteries	Aprotic	Aprotic	Aprotic	Alkaline/saline	Alkaline	Aprotic	Alkaline
Year invented	1996	2012	1966	1962	1878	2013	1968

[a] Oxygen inclusive.

1. Introduction

The ever-increasing global concerns over environmental and energy issues, such as air pollution, climate change and fossil fuel depletion has triggered substantial development of renewable energy technologies, including wind energy, solar, tidal/ocean currents, wave energy, bio-energy, geothermal and hydropower [1–3]. Replacement of fossil fuels by renewable sources of energy is one of the major challenges, which humanity has been facing during the last years. On the bright side, it is estimated that the world could possibly reach 100% renewable electricity by 2032 if the current installation rate of photovoltaic cells and wind power is maintained [4].

However, the intermittent nature of these sources has a significant impact on the operation, making the match between energy supply and demand difficult. To address these problems, low-cost, energy-efficient, safe and large-scale energy storage systems are needed [3,5]. It is essential to level off the variation in the grid and securing a reliable, steady and efficient energy supply [6–8].

Various types of electrochemical energy storage technologies, including, lithium (Li)-ion batteries [9–12], lead-acid batteries [13–20], metal-air batteries [21–25], redox flow batteries [5,26–30], fuel cells [31–36] and supercapacitors [37–42] have been developed. Nowadays, Li-ion battery is widely used; however, because of its low energy density and concerns over safety, researchers have been seeking for better replacements [9]. In this regard, metal-air batteries have drawn great attention due to their several advantages, such as low-cost, high theoretical energy densities and for some due to environmental benefits [43]. Various metals, such as Zn, Mg, Al, K, Na and Li can be used to fabricate rechargeable metal-air batteries. The theoretical energy density, voltage, specific capacity and electrolyte of the various metal-air batteries are summarized in Table 1.

Metal-air batteries have drawn special attention, because of their half-opened nature that uses inexhaustible oxygen from the air as oxidant, resulting in a high theoretical energy density [45]. Among them, the Zn-air batteries have so far received increasing attention because of their reasonable energy density in combination with a relatively low cost [46] and environmental friendliness as Zn is a nontoxic element. A typical Zn-air battery consists of four main components: an air electrode, membrane, an alkaline (concentrated KOH [47], NaOH [48] or LiOH [49]) electrolyte and a Zn negative electrode (Fig. 1). It has a theoretical maximum output voltage of 1.65 V based on the electrochemical reactions of oxygen reduction at the cathode and Zn oxidation at the anode under alkaline condition. The electrode reaction equations and their standard potential are shown below (R1-R4) [48,50,51].

Positive electrode: $O_2 + 2H_2O + 4e^- \leftrightarrow 4OH^-$ ($E^0 = +0.4$ V vs. SHE) (R1)

Negative electrode: $Zn + 4OH^- \leftrightarrow Zn(OH)_4^{2-} + 2e^-$ ($E^0 = -1.25$ V vs. SHE) (R2)

$Zn(OH)_4^{2-} \leftrightarrow ZnO + H_2O + 2OH^-$ (in the electrolyte) (R3)

Overall reaction: $2Zn + O_2 \leftrightarrow 2ZnO$ ($E_{cell} = E^{o}_{cathode} - E^{o}_{anode} = +1.65$ V) (R4)

The Zn-air system started to be commercialized in 1932 for hearing aids [52]. Mechanically rechargeable Zn-air systems showed significant progress in the 1990s. However, after about 50 years of intensive research, rechargeable Zn-air batteries are still in an early stage of commercialization because of various challenges, such as water evaporation, dendrite formation, atmospheric CO_2 reaction with OH^- ions and resulting in carbonate precipitation, lack of bifunctional air cathode (allowing both oxygen reduction and evolution reaction) and appropriate selective membrane [53]. Regarding the CO_2 contamination, it can have a large impact on battery performance. For example, the stability of bifunctional La0.6Ca0.4CoO3 oxygen electrodes for rechargeable Zn-air battery as a function of the CO_2 concentration in the feed gas has been investigated by Drillet et al. [54]. When air containing up to 1000 ppm was used as a feed gas, the oxygen reduction reaction (ORR) became life-limiting and run for only about 270 h (2500 h when pure oxygen as feed gas was used) due to pore clogging by carbonate precipitation. Similarly, 1% CO_2 in oxygen stream caused a drop in Ag/PTFE ORR electrode current density with time due to the formation of K_2CO_3 in the micropores [55]. To address these issues and endure the life and performance of Zn-air batteries, various strategies, such as passing the inlet air through a scrubber of alkaline filter materials or amines [56], replacing electrolyte to remove any accumulated carbonate [57], operating at higher temperatures to increase the solubility of carbonates and slow down its precipitation [44] and/or ionic liquids electrolytes which are CO_2-tolerant [58] have been suggested. However, it must be noted that most of these strategies result in much poorer battery performance. Moreover, the impact of CO_2 on AEM fuel cell performance has been reported to significantly decrease when operating

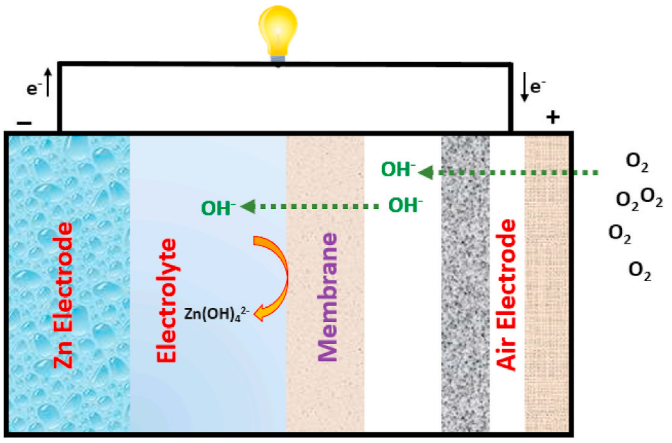

Fig. 1. A schematic diagram of alkaline Zn-air battery in discharge.

the cell at high current densities (above 1000 mA cm^{-2}) [59]. When a high current density was applied on the operating fuel cell, the OH^- ions formation at the cathode was increased. The OH^- ions are transported through the membrane, thus diluting the carbonate anions and consuming more CO_2 in the membrane. Similar high current densities operation technique might be used to avoid CO_2 effects in Zn-air batteries.

Recently, a number of research groups have been working to address these issues in order to realize rechargeable Zn-air flow batteries. This is clearly visible by the number of published papers in recent years (Fig. 2). The number of scientific publications in this field has revealed steady growth in the last 10 years, which points out that the Zn-air battery technology for energy storage is indeed a potential candidate attracting wide interest. The increasing attention to these batteries is attributable to the abundance and low cost of Zn [60] in combination with a relatively high energy density (theoretically 1087 Wh kg^{-1}, including the weight of oxygen in the capacity calculation), high safety and environmental friendliness [61]. Moreover, the battery generally exhibits a flat, constant discharge voltage and low equilibrium potential, which is an additional reason why it has received great attention [51]. Furthermore, Zn can be easily recycled using current recycling technologies [62].

Excellent reviews on the overall status and recent progress of Zn-air batteries exist in the literature [43,44,50,51,63–66], with the vast majority of research focused on the electrode materials and electrolyte (alkaline, acidic and neutral) components. In these studies, different air catalysts configurations, such as unifunctional ORR electrocatalyst, bifunctional air electrocatalysts and three-electrode configuration have been investigated. Moreover, the various groups of bifunctional catalysts, namely transition metal oxides, transition metals, carbon-based materials and precious metals/alloys, which are used in primary/secondary Zn-air batteries have been reviewed elsewhere [67].

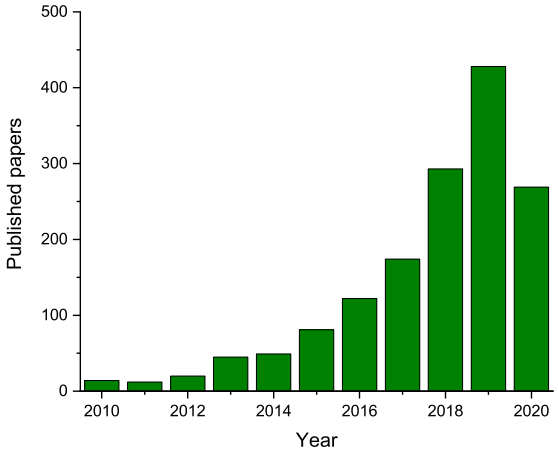

Fig. 2. Number of publications per year from 2010 to 2020 mentioning the term "Zinc/Zn-air battery" as derived from Web of Science database (accessed on June 22, 2020).

Due to the intense research efforts on the cathode electrocatalysts, the performance of Zn–air batteries is no longer limited by electrocatalysts and air electrode [68]. Various researchers have bypassed the cycling stability issue by adapting a three-electrode configuration, in which the oxygen evolution reaction (OER) and ORR electrodes are decoupled [69,70]. Therefore, a shift in a research direction from cathode electrocatalysts to the Zn negative electrodes has been suggested to truly commercialize this a century-old technology. However, in comparison to the other parts of the battery [71–77], the membrane has not yet received its deserved attention [78]. Therefore, the present review is focused on the membrane, which is a critical component of the Zn-air battery system. The main role of the membrane is to separate the electrodes, thus avoiding electrical short circuits, and to selectively conducting hydroxide (OH^-) ions from the air electrode to the Zn electrode and *vice versa* [79]. Additionally, it is very important to design a membrane that exhibits high structural resistance to avoid possible perforation by Zn-dendrites in order to assure the safety and long-term reliability of the battery [44,80]. Zn-dendrites growth retarding membranes are discussed in section 4.

There are several partially contradicting requirements for an appropriate membrane to be used in rechargeable Zn-air batteries. The membrane should exhibit high chemical and electrochemical stabilities in an oxidative medium [81,82], a high ionic conductivity and should be able to swell in the electrolyte [51,81] without compromising its mechanical robustness. The membrane should also reduce the crossover of zincate ($(Zn(OH)_4^{2-})$ ions [83–85]. Moreover, the membranes should be manufactured at an acceptable cost. The key requirements of membranes to be applied in high-performance Zn-air battery systems are discussed in detail in section 2.

Most of the membranes currently used in Zn-air batteries i.e., porous membranes, have been adapted from Li-ion and nickel batteries. Despite the relatively good chemical stability and low costs of these commercial membranes, such as Celgard® 4560 and Celgard® 5550 (Celgard LLC), a crossover of significant amounts of $Zn(OH)_4^{2-}$ species from the Zn electrode to the air one has been reported to increase cell polarization and resulting in capacity fading of the battery (section 2.3) [83,86,87]. This indicates the need for designing and developing dedicated membranes that can block zincate permeation in order to achieve a highly-effective rechargeable Zn-air flow battery [83,84,86].

To address this challenge, various types of membrane chemistries, including anion or cation-exchange membranes (AEM/CEMs), composite membranes and electrospun nanofiber membranes have been explored. Each of these membranes has different sets of advantages and drawbacks, which influence the performance of Zn-air batteries. In conventional batteries, the term "separator" is often used to refer to a porous membrane, which mechanically separates two compartments without functionality, imbibed with electrolytes [88]. Moreover, in the literature, the terms membrane, separator and membrane separator have been used interchangeably. To avoid a possible misinterpretation, the basic definition and classification of the term "membrane" is revised more closely here. A membrane can be defined as a permselective barrier material between two phases [89] that allows some species to pass while preventing others on application of a transmembrane driving force [90,91], which could be a hydrostatic pressure gradient, vapor pressure gradient, electrical potential gradient or concentration gradient [92]. Based on their morphology, membranes can be classified into two main categories of porous and non-porous (dense) [93]. Porous membranes, which are made up of a solid matrix with defined pore sizes varying from 0.2 nm to about 20 μm [94] separate target solutes mechanically by their size exclusion, whereas in non-porous membranes transport occurs by a solution-diffusion mechanism [95] inside the membrane. Porous

membranes can be further referred to as macroporous (average pore diameters larger than 50 nm), mesoporous (average pore diameters between 50 and 2 nm) and microporous (average pore diameters between 2 and 0.2 nm) according to the classification adopted by the IUPAC [96].

For this reason and to avoid confusion, only the term membrane will be used throughout the present treatise, which, to the best of our knowledge, is the first review on the state-of-the-art membranes used in Zn-air batteries. The properties and performance of seven types of membranes used in Zn-air batteries (following a classification done on the basis of their composition and structure), namely porous polymeric membranes prepared by phase inversion and electrospinning, modified porous membranes, ion solvating membranes, AEMs, CEMs and inorganic membranes are discussed and compared. The existing research gaps and strategies proposed to solve the problems associated with the currently used membranes are also discussed.

2. Performance determining properties of membranes in zinc-air batteries

2.1. Chemical and electrochemical stability

The most commonly used electrolytes in Zn-air batteries are aqueous alkaline (KOH or NaOH) solutions because of the higher stability of Zn in alkaline media and the use of non-noble catalyst in air electrodes. Usually, KOH has been used as the electrolyte in Zn-air batteries because of its higher ionic conductivity, higher oxygen diffusion coefficients, and lower viscosity compared to that of NaOH [97]. The specific conductivity of an aqueous KOH electrolyte depends on its concentration and temperature. Generally, the conductivity of the electrolyte increases up to a certain concentration and then it decreases due to an increase of viscosity and lower dissociation due to lack of water and formation of ion pairs, precipitates, etc. An increase in viscosity decreases the mass transport rate of OH^- ions [98–100]. For this reason, 6 M KOH solution is most commonly used to provide both an appropriate ionic conductivity and viscosity [100,101].

The chemical stability of membranes in such a highly alkaline harsh environment is critical since the OH^- ions, which are strong nucleophilic bases, could degrade the membrane. In a study done by Sapkota and Kim [79], microporous synthetic resin filters (Yumicron MF-250), cotton cloths, polyimide-based nylon net filter and polypropylene resin membrane were tested in a Zn-air fuel cell. Despite the known resistance of the cotton cloths and Yumicron MF-250 to alkalis, the membranes were reported to be stiffened and easily fractured, whereas the polypropylene resin membrane and Nylon net filter showed a good stability. However, the mechanisms responsible for the degradation of the membranes used were not identified.

The alkaline stability of a membrane is usually determined by comparing its chemical structure, mechanical properties and/or performance (e.g., conductivity) before and after immersing into an alkaline media (e.g., 2 M KOH solution at 60 °C), for defined time. A decrease in ionic conductivity and/or ion-exchange capacity with immersion time indicates degradation of functional groups.

The alkaline stability issue is more critical when AEMs are used since most of their functional groups are prone to a nucleophilic attack. The alkaline stability/degradation of AEMs is well-reviewed in the literature [102–107]. Operations under electrical current flowing conditions make the chemical stability problem more complicated as a result of a possible formation of free radicals. Therefore, a membrane with a high stability in the alkaline solution, which withstands during electrochemical operations is required [79]. For instance, commercial porous membranes based on polyolefins (e.g., polypropylene, polyethylene), such as Celgard® 3501 and 5550, and inorganic membranes are known for their good alkaline chemical stability. Similarly, the commercial CEMs based on a perfluorosulfonic acid polymer i.e. Nafion® has a good chemical stability.

2.2. Conductivity

Hydroxide conductivity has a major influence on the performance of Zn-air batteries. A membrane with a high OH^- ion conductivity is desirable since a low resistive OH^- ion transport allows high conversion rate of the electrochemical reaction. As the OH^- mobility through the membrane must be as high as possible, the formation of swelling nanochannels in the membrane thickness is very important. Due to the larger size (1.6 x) and, thus, lower diffusivity of OH^- ions compared to that of H^+ ions, the rate of OH^- transport is expectedly lower than that of H^+. However, it must be noted that the transport easiness of OH^- is not only associated with its size, which is important for diffusion process, but also with its transport via Grotthuss mechanism [108–110].

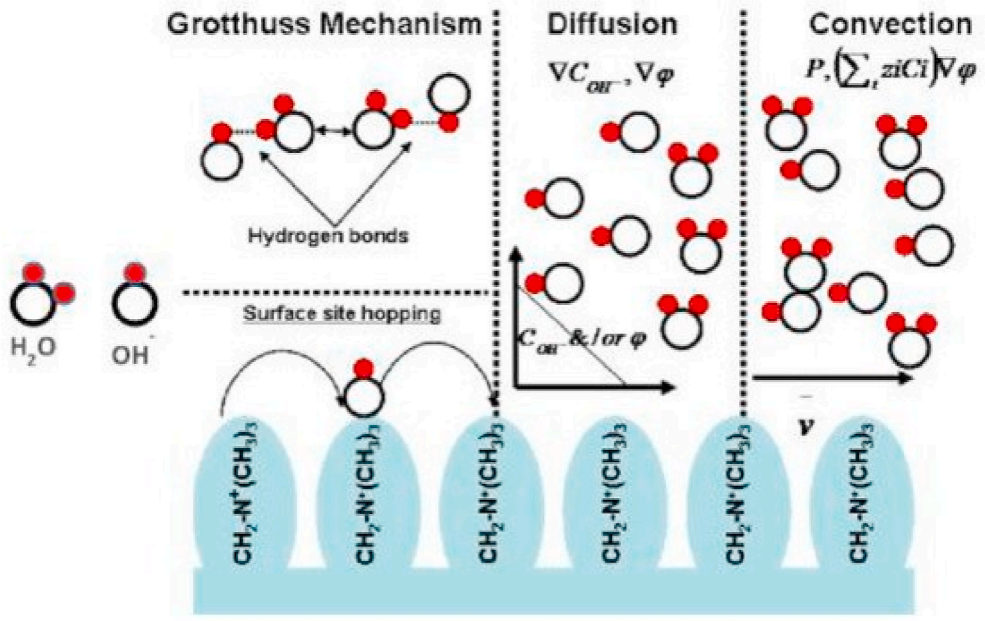

Scheme 1. Dominant transport mechanisms for hydroxide ions in AEMs. Reproduced with permission from Ref. [110]. Copyright 2010, The Electrochemical Society.

Understanding the transport mechanism of OH^- ions is important in order to increase the OH^- ion conductivity. The transport mechanisms of hydrated OH^- ions in aqueous solution have been discussed elsewhere [111,112]. It is considered that OH^-(aq) exhibits a nonclassical, hypercoordinated solvation structure. The main transport mechanisms of OH^- ions through AEMs that have been proposed in the literature are schematically shown in Scheme 1. Similar to the transport of proton in proton exchange membranes, Grotthuss and vehicle mechanisms are believed to be the dominant OH^- transport mechanisms through membranes [110,113]. In Grotthuss mechanism, the OH^- ions transports from one water molecule to the next via hydrogen-bonding [111–115]. In addition to the membrane properties, the operating conditions, such as temperature and relative humidity affect the OH^- mobility through a membrane. The OH^- ion conductivity increases with increasing temperature and relative humidity. The increment in ionic conductivity of the membrane with the temperature increasing can be explained for two reasons: The trend can be explained by faster OH^- ions motion [116] and wider ion transport channels [117] at an elevated temperature.

Surface site hopping is another mechanism discussed in the literature as a possible OH^- ion transport in the membrane. It involves the movement of hydroxide ion by hopping between strongly interacting groups in the polymer chain [105,110,118]. In this mechanism, the $-N^+OH^-$ grafted functional group is solvated and dissociated by water molecules. Subsequently, the OH^- ion is attracted by the adjacent cationic chain, then the process repeats. The distance between the neighboring functional fixed groups and the ion exchange capacity influence the transport rate of OH^- ions via the surface site hopping mechanism.

On the other hand, the conductivity of non-functionalized porous membranes depends on their electrolyte wettability. The wettability of porous membranes depends on the polarity and tortuosity of the membrane porous structure. For instance, some Celgard® membranes are treated with a (cationic/nonionic) surfactant to increase their hydrophilicity leading to higher electrolyte uptake. This has been discussed in section 3.1.3.2.

Ionic conductivity of gel-polymer electrolyte membranes is achieved by the transport of salt ions through the water [119]. In other words, the conductivity is mainly related to the water diffusive motion across the membrane. In such membranes, ions motion paths can be eventually blocked by the ions aggregation unless the salt concentration is optimized [120]. Another challenge associated with gel-polymer electrolyte membranes is the progressive loss of electrolyte, which leads to an increasing ohmic resistance and decline of the battery performance [121]. One option to address this issue is to fix the functional charged groups functions on the polymer backbone, as it is done in ion-exchange membranes.

The OH^- conductivity (σ) of a membrane can be measured by impedance spectroscopy [117,122]. Usually, fully hydrated membranes (in OH^- form) are sandwiched in a Teflon cell equipped with Pt foil contacts. The in-plane ionic conductivity, in mS/cm, of a sample is calculated from equation (1):

$$\sigma\ (\mathrm{mS/cm}) = \frac{L}{R\ x\ A} \quad (1)$$

where L (cm) is the distance between electrodes (thickness of the membrane), R is the resistance of the membrane (Ω) and A is the cross-sectional area of the sample (cm^2).

2.3. Selectivity and permselectivity

Another important membrane requirement for rechargeable Zn-air batteries is its selectivity. In strong alkaline solutions, OH^- reacts with Zn^{2+} and forms $Zn(OH)_4^{2-}$ [44,50] via a number of elementary first-order reactions [123,124] (Equations R5-R6). The membranes need to be selective for OH^- ions, without any crossover of $Zn(OH)_4^{2-}$ formed in the Zn electrode compartment [44,51]. In practice, $Zn(OH)_4^{2-}$ crossover is a common problem as it is able to cross due to the concentration gradient, especially when porous membranes are used. Therefore, to address the crossover of $Zn(OH)_4^2$ ions issues, a membrane that is able to block the transportation of $Zn(OH)_4^{2-}$ ions without significantly affecting the OH^- ions transportation would be one major requirement to achieve a long cycle life.

$$Zn + OH^- \leftrightarrow Zn(OH) + e^- \quad (R5)$$

$$Zn(OH) + OH^- \leftrightarrow Zn(OH)_2^- \quad (R6)$$

$$Zn(OH)_2^- + OH^- \leftrightarrow Zn(OH)_3^- + e^- \quad (R7)$$

$$Zn(OH)_3^- + OH^- \leftrightarrow Zn(OH)_4^{2-} \quad R8)$$

Due to the low solubility of ZnO at the air electrode, the $Zn(OH)_4^{2-}$ to ZnO conversion ($Zn(OH)_4^{2-} \rightarrow ZnO\ (s) + H_2O + 2OH^-$) is accelerated, resulting in the formation of resistive ZnO layers. This leads to a loss of battery capacity with cycling [85]. Moreover, ZnO powders could clog the porous air electrode, resulting in large cell polarization [125]. Thus, $Zn(OH)_4^{2-}$ crossover could affect the durability of the battery by decreasing its lifespan. This indicates the substantial need for avoiding $Zn(OH)_4^{2-}$ ions crossover [83]. One possible way is by using a porous membrane with a proper pore size and porosity. Another method that has been widely proposed to solve the problem is to use an AEM that has well-defined and controlled ionic nanochannels [44,63]. Moreover, different membrane surface modifications techniques could also be performed to minimize the permeation of $Zn(OH)_4^{2-}$ ions.

On the other hand, the size of the $Zn(OH)_4^{2-}$ anionic complex consisting of four OH^- groups and a Zn^{2+} cation is far larger than that of a single OH^- anion. The solvodynamic radius of the $Zn(OH)_4^{2-}$ ion in 4 M NaOH and at 25 °C was reported to be 3.41 Å [126]. The Stokes radii were reported to decrease with increasing alkali concentration, due to the competition between solvation of $Zn(OH)_4^{2-}$, Na^+, and OH^- ions by water molecules. Here, the ionic radius of $Zn(OH)_4^{2-}$ is assumed to be the same as the ionic radius of Zn^{2+} [90,91] i.e., much higher than that of OH^-. The relative diffusivity easiness of OH^- ion compared to that of the $Zn(OH)_4^{2-}$ ion is favoring the OH^- transport across the membrane [83]. Table 2 presents the ionic Stokes radii of the different species involved (OH^-, Zn^{2+} and $Zn(OH)_4^{2-}$) and their diffusion coefficients at infinite dilution at 25 °C. Depending on the electrolyte used (KOH or NaOH), K^+ or Na^+ will be present, whereas CO_3^{2-} is due to the possible carbonation unless the CO_2 is removed, as the air electrode is open to the air.

A simple diffusion cell composed of two chambers, separated by a membrane, filled one side with a KOH electrolyte solution (a typical example is, 6 M, 100 mL) and $Zn(OH)_2$ and a second side with only a KOH (6 M, 100 mL) solution is usually used to determine the diffusion coefficient of $Zn(OH)_4^{2-}$ ions through the membrane. This is similar to the method employed to determine the vanadium ion crossover in Vanadium redox flow battery [131–133]. However, it should be noted that this procedure does not compensate for ionic strength. Best practice procedure would be to use a non-active ion (e.g., $Mg(SO_4)$ in the case of Vanadium) to compensate for the loss in ionic strength and to exclude osmotic pressure as an additional driving force. The change of concentration of $Zn(OH)_4^{2-}$ ions with time is usually monitored using elemental analysis methods, such as inductively coupled plasma atomic emission

Table 2
Ionic Stokes radii and diffusion coefficient (D) of species involved in Zn-air battery at 25 °C.

Species	Ionic Stokes radii (Å) [127]	D (10^{-9} m^2 s^{-1}) in water [128–130]
OH^-	0.46	5.27
K^+	1.25	1.96
Na^+	1.84	1.33
CO_3^{2-}	2.66	0.96
Zn^{2+}	3.49	0.72

spectrometry (ICP-OES) [83,85,86], ICP-mass spectroscopy (ICP-MS) [134], polarographic response [135], or complexometric titrations [136]. To avoid a long experimental period and sample post-processing steps associated with ICP-MS analyses, an anodic stripping voltammetry (ASV) sensing platform which provides real-time concentrations of Zn $(OH)_4^{2-}$ crossing the membrane has been reported [136]. The diffusion coefficient (D, $m^2\ s^{-1}$) of $Zn(OH)_4^{2-}$ ions can be calculated using a mass balance equation:

$$V_B\frac{dC_B(t)}{dt}=\frac{DA}{L}(C_A-C_B(t)) \quad (2)$$

which after integration (by assuming V_B to be constant) can be rearranged as:

$$ln\left(\frac{C_A}{C_A-C_B}\right)=\frac{DA}{V_BL}t \quad (3)$$

where A and L are the effective area (m^2) and thickness (m) of the membrane, respectively; V_B is the volume of the depleted side and t is the elapsed time (s). C_A (mol L^{-1}) and C_B (mol L^{-1}) are the concentrations of $Zn(OH)_4^{2-}$ in the enriched and depleted chambers, respectively. As an example, the dependence of the $Zn(OH)_4^{2-}$ ion diffusion coefficient on NaOH concentration (1–4 M) and temperature has been reported elsewhere [126].

Another important parameter which should be taken into consideration is the permselectivity (S cm s^{-1}) of the membrane, which can be calculated as the ratio of hydroxide conductivity (σ (OH^-), mS cm^{-1}) to $Zn(OH)_4^{2-}$ diffusion coefficient (D ($Zn(OH)_4^{2-}$), $cm^2\ s^{-1}$) [85]. Permselectivity indicates the preference of the membrane for OH^- ions over Zn $(OH)_4^{2-}$ ions. Therefore, in practice, this parameter should be taken into consideration when selecting a suitable membrane for a specific application. For instance, a porous membrane, such as Celgard® 3501, might have a high hydroxide ion conductivity but exhibits also a high crossover of zincate ions. On the other hand, an AEM could have a comparably acceptable hydroxide ion conductivity, but offer much better zincate ions retention. In this case, the membrane permselectivity can be used as the final decision factor to select the most appropriate membrane.

2.4. Mechanical strength

The membranes must be mechanically robust to withstand the tension of winding operation and stacking stress during continuous cell assembly. For a stable and long battery lifespan, an optimal and uniform membrane thickness is required [137]. Usually, thin membranes have lower internal resistance, but a small thickness can have a negative impact on the mechanical strength. On the other hand, thicker membranes are generally less prone to fail mechanically, which improves better battery safety. However, the internal resistance increases with increasing thickness, and the mechanical robustness on one hand must therefore be balanced against the ohmic resistance on the other. The typical thickness of membranes used for rechargeable batteries is reported to lie between 20 and 50 μm [138].

Mechanical properties of a polymeric membrane are dependent of its elastic modulus, tensile strength and ductility [139]. Typical mechanical strength values of commercial Celgard® membranes have been summarized in Ref. [140,141]. The minimum requirement of puncture (i.e., the maximum load required for a given needle to puncture a membrane) and mechanical strengths for a 25 μm thick membrane is 300 g and 1000 kg cm^{-2}, respectively. Trilayer structured (PP/PE/PP) Celgard® membranes display exceptional puncture strength, whereas AGM membranes exhibit a low puncture resistance [141].

2.5. Water uptake and anisotropic swelling ratio

The membrane should possess optimized water retention capacity in order to facilitate the mobility of OH^- ions and to avoid drying out by evaporation since the air electrode is exposed to the atmosphere [142]. Compared to other types of aqueous batteries, in which in general both sides of the membranes are in contact with aqueous electrolytes, Zn-air batteries are usually half-closed system, in which only one side of the membrane is in contact (immersed) in the aqueous alkaline solution, whereas the other side of the membrane is contacted to a gas-diffusion electrode, the system is therefore asymmetric. The air electrode has to maintain its hydration even during the discharge process and water consumption associated with O_2 reduction.

The water consumption due to both electrochemical reactions and electro-osmosis can induce electrode or/and AEM drying out, membrane shrinking and lead to a shortened battery lifespan. Moreover, the membrane may undergo mechanical stress and deformation from the volume expansion of the Zn electrode due to the formation of oxidized Zn species. This can lead to ineffective interfacial contact between the electrode and electrolyte. Thus, the active materials become less accessible to the ionic species. Accordingly, the anisotropic swelling ratio of the membrane is another crucial parameter that affects the Zn-air battery cycling performance [142–145]. An anisotropic swelling degree is defined as the ratio of through-plane swelling to in-plane swelling of the membrane [146]. A membrane with a low anisotropic swelling degree, combined with high water retention and OH^- conductivity is expected to improve the specific capacity and the cyclic stability of the battery [142]. On the other hand, membrane with high anisotropic swelling degree, for instance, the A201®-based Zn-air batteries exhibited a rapid voltage and capacity loss after some cycles, which was attributed to the progressive loss of water and ionic conductivity in the membrane during the constant current conditions applied [142–145].

3. Classification of membranes used in zinc-air batteries

The membranes used in Zn-air batteries can be classified into seven major types: (a) phase inversion polymeric porous membranes, (b) electrospun nanofiber membranes, (c) modified porous membranes, (d) inorganic membranes, (e) AEM, (f) CEM and (g) ion solvating membranes (also called gel polymer electrolyte membranes) depending on their composition and structure (Scheme 2). The first sub-section 3.1.1 is devoted to polymeric porous membranes prepared by the phase inversion method, since they are the most commonly used ones. On the other hand, the nanofiber membrane is another group of porous membranes prepared by an electrospinning technique presented in sub-section 3.1.2. The next sub-section 3.1.3 focuses on modified porous membranes. In this section, strategies followed to improve the properties of porous membranes are discussed. A brief discussion on inorganic membranes is presented in section 3.1.4. Finally, in section 3.2, dedicated to polymer electrolyte membranes, AEMs, CEMs and ion solvating membranes are discussed in sub-sections 3.2.1, 3.2.2 and 3.2.3, respectively.

3.1. Porous membranes

3.1.1. Phase inversion membranes

The early development of Zn-air batteries was limited by the lack of suitable membranes. As a result, inorganic filter paper (Whatman) impregnated with poly vinyl acetate (PVAc) aqueous solution (24 wt%) [147,148] and porous membranes [79] developed for other applications were used. In the latter work, the performance of various porous membranes was compared in a Zn-air fuel cell. An Yumicron MF-40 (pore size of 0.4 μm) membrane was reported to have lower performance in terms of cell voltage than Yumicron MF-250 (pore size of 2.5 μm).

Later on, nonwoven porous membranes made of polyethylene (PE), poly(vinyl alcohol) (PVA), polyamide, poly(etherimide) (PEI), poly (acrylic acid) (PAA) and polypropylene (PP) have been commonly used

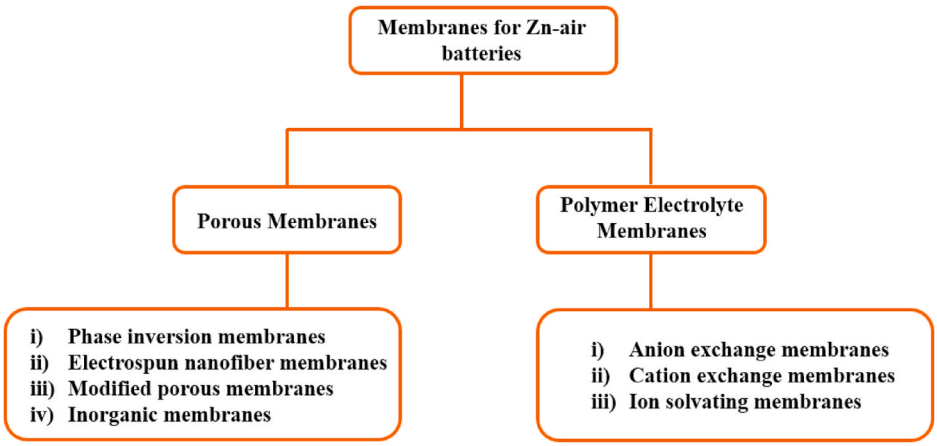

Scheme 2. Classification of membranes used in Zn-air batteries based on their composition and structure.

in Zn-air batteries [48,84,149]. Nowadays, commercial membranes with a well-defined porous structure, such as Celgard® 5550 [149], which has a PP/PE/PP trilayer structure are commonly used in Zn-air batteries. The PP is used to maintain the integrity, providing mechanical support to avoid internal shorting, whereas the core PE due to its low melting point is able to shut down when the battery is overheated [149] since the PE layer melts and closes the film pores, thus blocking ions migration [150]. These laminated porous membranes are prepared via a dry process i.e., the polyolefin is melted, thermally annealed to increase the size and amount of lamella crystallites, and then precisely stretched to form tightly ordered meso-pores, which are usually coated with surfactants to increase water-based electrolyte wettability [140,149]. The closely ordered nature of the meso-pores of these membranes allows them to be highly OH^- ion conductive [44,149,151]. For instance, Celgard® 3501 was reported to have an OH^- conductivity of 12.8 mS cm^{-1} and 80.1 wt % KOH solution (6 M) uptake at room temperature [86].

The porous membranes commonly used (PP-based) in rechargeable batteries have an average pore size which is much larger than the size of solvated zincate ions, which results in their crossover. For example, Celgard® 5550 has an average pore size of 100 nm [152], 64 nm [153] (according to Manufacturer's datasheet), which is much larger than the size of zincate ions. Therefore, the $Zn(OH)_4^{2-}$ species are able to diffuse across them to the air electrode [83,154]. Significant zincate ions crossover has been reported in a number of studies when such porous membranes were used [83,85,86,155]. The diffusion coefficient of zincate ions through Celgard® 3501 and Celgard® 5550 was reported to be 3.2 x 10^{-11} [85] and 1.1 x 10^{-5} m^2 s^{-1} [83], respectively. This is a very large difference in the zincate ions diffusion coefficient value despite the fact that both membranes have exactly the same porosity (55%) and pore size (64 nm) [153]. The notable difference between the two membranes, which might explain the large difference in zincate ion diffusion, is that Celgard® 3501 is only coated, whereas Celgard® 5550 is laminated and coated membrane [153]. The use of two Celgard® 3401 membranes (50 nm pore size) together was reported to have a lower zincate ions diffusion coefficient (6.9 x 10^{-12} m^2 s^{-1}) [156]. To improve the performances and avoid the crossover of $Zn(OH)_4^{2-}$ ions, a membrane with pores that are large enough to permit the OH^- ions but small enough to prevent the permeation of $Zn(OH)_4^{2-}$ ions is required [51].

Other membrane materials, including cellulosic films, such as cellophane, have also been investigated in Zn-air batteries [157,158]. The diffusion coefficient of zincate ions for cellophane® 350PØØ membranes (unsoften cellulose film) (Innovia Films Company), wet ionic resistance of > 96.8 mΩ cm^2 using 40% KOH [159], was measured using anodic stripping voltammetry (ASV) [136]. The cellophane membrane (6.7×10^{-12} m^2 s^{-1}) was found to have a lower zincate crossover than that of Celgard® 3501. The diffusion coefficient of $Zn(OH)_4^{2-}$ through Celgard® 3501 reported in this study was coherent with the value discussed previously in Ref. [85]. The cellophane membrane's diffusivity to $Zn(OH)_4^{2-}$ was reported to be similar (3.7×10^{-12} m^2 s^{-1}) in another study [157]. It should be noted that cellophane typically has a less porous (about 3–10 nm [160]) structure and is more negatively charged than that of Celgard® 3501 [161]. Thus, the smaller and (negatively) charged pores of the cellophane were thought to be more selective in excluding the negatively charged $Zn(OH)_4^{2-}$ ions. A contradictory result was reported in another study, in which a cellophane membrane was reported to show no zincate blocking effect at all when used in Zn/MnO_2 cell [162].

In addition to commercial porous membranes, various composite porous membranes have been reported in the literature. Phase inversion is a process, in which a homogeneous polymer solution (polymer and solvent) casted on a suitable support is immersed in a coagulation bath containing a nonsolvent (usually water) and is converted into two phases (polymer-rich and liquid-rich phases) [163–165]. Phase inversion has been so far the most commonly used method to prepare (porous) membranes due to its simple processing and flexible production scales [166,167]. Porous membranes used so far in Zn-air batteries are presented in Table 3.

Wu et al. [168] prepared PVA/poly(vinyl chloride) (PVC) porous membrane and studied its potential electrochemical performance on a secondary Zn battery. The PVA and PVC polymers were dissolved in water, and the dried composite PVA/PVC film was immersed in THF in order to form a macroporous structure (pore size range of 60–180 nm) via a partial dissolution process. This allowed a high KOH electrolyte uptake by the membrane. The membrane pore size and its distribution were controlled by varying the amount of PVC, the partial dissolution time and the etching temperature. The PVA/PVC-based secondary Zn battery exhibited a stable charge potential. This was claimed to be due to the high ionic conductivity (37.1 mS cm^{-1} at 30 °C for PVA/10 wt% PVC) and macroporous structure of the membrane. As a result, the cell potential during the charge period was much less polarized; thus, the current efficiency (70–80%) and the life-span (50 cycles) of the battery were improved.

Moreover, solid PVA/PAA membranes with a uniform structure were prepared via a solution casting method [169]. The room temperature ionic conductivity of these membranes reached 140–300 mS cm^{-1} depending on the ratio of PVA to PAA. The ionic conductivity of membranes was reported to increase with the increase of PAA content. The percent utilization of the Zn-air cell capacity was as high as 90% when the PVA/PAA (10:7.5) membrane was used and the cell was discharged at a C/10 rate. The power density was reported to reach 50 mW cm^{-2}.

3.1.2. *Electrospun nanofiber-based membranes*

Electrospinning is a versatile membrane preparation technique widely used to produce membranes with large specific surface area and

Table 3
Performance of porous polymeric phase inversion membranes used in Zn-air batteries.

Membrane	Preparation method	Characteristics	Cell type and conditions	Electrodes	Electrolyte	Performance	Ref.
Celgard® 3501	Commercial (Celgard LLC)	Porosity* = 55%, pore size* = 64 nm Thickness: 24 μm	Rechargeable Zn–air battery	Zn electrode: Zn-based gel (Zn powder, PAA and 6 M KOH electrolyte solution) Ni foil: current collector Air electrode: commerciale (ADE75 (catalyst = Co_3O_4), MEET)	6 M KOH electrolyte solution	-Discharge capacity (2nd cycle) ~34 mAh g_{Zn}^{-1} -Pinwheel connected to Zn–air cell stopped after about18 min	[85]
Celgard® 5550	Commercial (Celgard LLC)	Porosity* = 55%, pore size* = 64 nm Thickness: 25 μm	Rechargeable Zn–air battery	Zn electrode: pure Zn plate Air electrode: Pt and Ir carbon composite	6 M KOH aqueous solution	-Initial (59.4%) and final (51.2%) energy efficiencies -Coulombic efficiency (99.8%). −37 cycles	[83]
Celgard® 3401	Commercial (Celgard LLC)	Porosity* = 41%, pore size* = 43 nm Thickness*: 25 μm	Zn-air fuel cell	Zn electrode: Zn powder Air electrode: MnO_2 powders was used as the catalytic material.	carboxymethyl cellulose with 8 M KOH solution.	-Discharge current (mA) = 500 mA, at constant 0.7 V for 40 min using flowing KOH solution.	[170]
PVA/PVC	Solution casting method and a partial dissolution process	Pore size: 60–180 nm Thickness: 150–200 μm	Rechargeable Zn electrodes Galvonostatic charge/discharge measurements were carried out at a C/10 charge rate and a C/5 discharge rate.	Zn electrode: ZnO and $Ca(OH)_2$ 2 wt% of Cu conductive nanopowders	8 M KOH aqueous solution.	-Specific discharge capacity: 353 mAh g_{Zn}^{-1} for 45 cycles -Coulombic efficiency: 70–80% -Effectively prevented any Zn dendritic formation. -Life cycle reached over 50 cycles	[168]
PVA/PAA	Solution casting method	ionic conductivity 301 mS/cm room temperature and 32 wt% KOH solution (PVA:PAA = 10:7.5 sample)	Zn-air cell BAT 778 model charge/discharge unit The discharge curves: C/10 discharge rate at 25 °C	Zn powder gel: Zn powder, carbopol 940, 32 wt% KOH and additives Ni-foam current collector GDL: carbon slurry	32 wt% KOH	PVA/PAA (10:7.5) membrane: -Discharge current (mA) = 150, 8.98 discharge h and -Utilization (%) = 89.8 -Power density: 50 mW cm^{-2}	[169]
PEO/PVA	Solution-cast technique	Average pore size (175 nm) ionic conductivity:153 mS cm^{-1} tensile strength 0.76 MPa.	Zn-air battery discharged at room temperature with the *C*/10 rate	Zn electrode: mix of Zn powder and Polyvinylidene fluoride (PVDF) Air electrode: -carbon slurry for the active layer of the air electrode was prepared by mixing of acetylene black, $KMnO_4$, Carbon black (Vulcan XC-72R), Na_2SO_4 and PVDF	KOH	Discharge curve: 0–25 min: the voltage falls abruptly to an OCV (1.10 V). 25–510 min: voltage drops to 0.55 V. 510–560 min: the rate of discharge starts accelerating (voltage decline to 0.3 V)	[82]
PVA/poly (epichlorohydrin) (PECH)	Solution-cast technique	Ionic conductivity: 10^{-2} - 10^{-3} S cm^{-1} at room temperature when the blend ratio is varied from 1:0.2 to 1:1.	Solid-state Zn–air battery discharged at the C/10 rate at 25 °C	Zn powder gels: Zn powder, Carbopol 940 gelling agent, 32 wt% KOH and some metal additives Carbon slurry for the gas-diffusion acetylene black and 30 wt% PTFE (teflon-30 suspension) as a binder Ni-foam current-collector	32 wt% KOH	PVA/PECH (1:0.2) membrane: -Cell utilization 86% -C/10, 150 mA, 8.59 h	[171]

*Manufacturer datasheet [153].

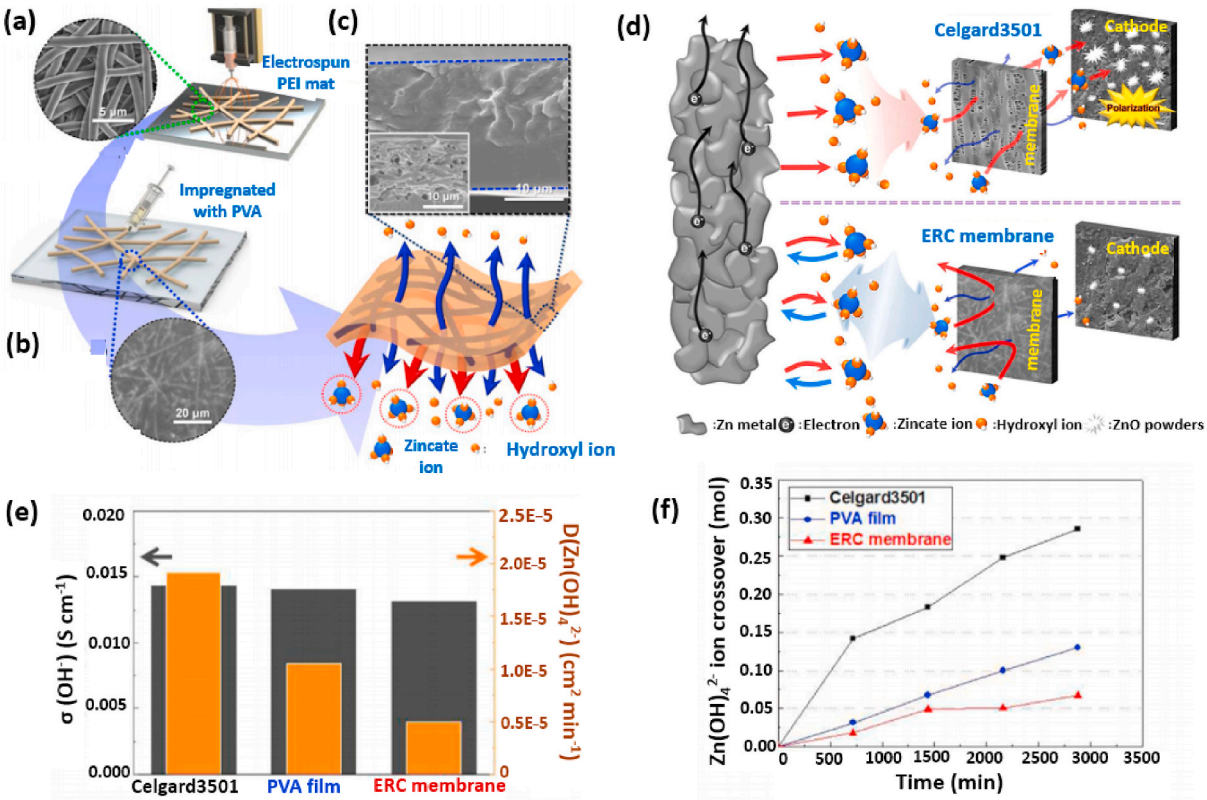

Fig. 3. Preparation of ERC membrane and characterization of Celgard® 3501, Pristine PVA film and ERC membrane: (a) electrospun PEI nanomat; (b) impregnation of PEI nanomat with PVA; (c) Cross-sectional SEM of ERC membrane and an illustration showing its permselective transport behavior; (d) illustration of permselectivity of ERC and Celgard® 3501 membranes; (e) OH^- conductivity ($\sigma(OH^-)$) and ($D(Zn(OH)_4^{2-})$); (f) $Zn(OH)_4^{2-}$ ions across the membranes (mol). Reproduced with permission [85]. Copyright Elsevier 2015.

small fiber diameter and pore size [172–174]. Membranes prepared by this method are referred to as electrospun nanofiber membranes [175]. The entangled fibers provide integrity and mechanical strength to these membranes. Non-woven mat membranes are commonly used in Li-ion [176,177], lead-acid [178] and in some types of alkaline [149] batteries. High electrochemical performances [172] and oxidation stability [173] were reported in Li-ion polymer batteries using such membranes. Recently, few electrospun-based nanofibrous membranes have been reported in the literature and have been tested in Zn-air battery applications.

Membrane-based on syndiotactic polypropylene (syn-PP) nanofibers were prepared using electrospinning [179]. Granular syn-PP was dissolved in a mixture of decalin, acetone and DMF and the resulting solution (7.5 wt%.) was electrospun (Potential: 10.5 kV; distance: 15 cm; flow rate: 0.8 mL h^{-1}). The syn-PP nanofibers (coated with PVAc glue)-based Zn-air battery was found to exhibit more than 40% discharge capacity improvement compared to the Whatman filter paper-based battery. The improvement in the performance of the batteries was attributed to the membrane non-ordered and layered-fibrous structures.

A promising electrospun nanofiber mat-reinforced composite membrane (ERC) for Zn-air battery was reported by Lee et al. [85]. The membrane was fabricated by impregnating KOH liquid electrolyte-swollen PVA into PEI nanofiber mats (referred to as ERC membrane, with a thickness of 27 ± 5 μm). Fig. 3 represents the electrospun PEI nanomat (a) and impregnation of PEI nanomat with PVA (b), respectively. Here, the PEI nanofiber provides a mechanical strength and dimensional stability, whereas the relatively entangled electrolyte swollen PVA is believed to allow the small-sized OH^- and prevent the bulky zincate ions passage. This unusual OH^- permselective transport behavior of the electrospun composite membrane is illustrated schematically in Fig. 3 (c and d).

The prepared composite membrane and reference membranes (PVA film and Celgard® 3501) used were compared in terms of OH^- ions conductivity, $Zn(OH)_4^{2-}$ ions crossover (in mol min^{-1}) and permselectivity. The $Zn(OH)_4^{2-}$ ions diffusion coefficient of the ERC membrane was four times lower than that of Celgard® 3501 membrane (Fig. 3e and 3f), which induced a better permselectivity of OH^- ions over $Zn(OH)_4^{2-}$ ions (1.7×10^{11} vs. 6×10^9 S s m^{-3}). This better permselectivity improved the cycle capacity retention of Zn-air batteries, since the 2nd discharge capacity of the ERC-based cell was about 7 times higher than that of the Celgard® 3501 membrane (~213 vs. ~34 mA h g^{-1}).

3.1.3. *Modified porous membranes*

To prevent the permeation of $Zn(OH)_4^{2-}$ ions through porous polymeric membranes, further optimization of these membranes have been achieved through surface modification approaches, which can be classified into two broad categories as nanoparticle-filled (composite) membranes and ion selective polymer-coated membranes.

3.1.3.1. Composite membranes. One possible method to minimize the crossover of $Zn(OH)_4^{2-}$ species is by plugging the pores of the porous membranes using inorganic particles. The preparation of composite membranes can involve incorporation of inorganic nanoparticles into the polymeric matrix during the fabrication process or filling/coating of a porous membrane with particles once the membrane is prepared. In both cases the aim is to prevent passage of zincate ions [180]. These techniques have been extensively investigated also for other batteries, such as Li-ion batteries. Similarly, pore filling with inorganic salt containing fluoride ions has been employed in cross-linked PVA-based membranes and used for a silver-Zn battery [181]. The fluoride salt due to its relative insolubility is expected to remain in the polymer gel.

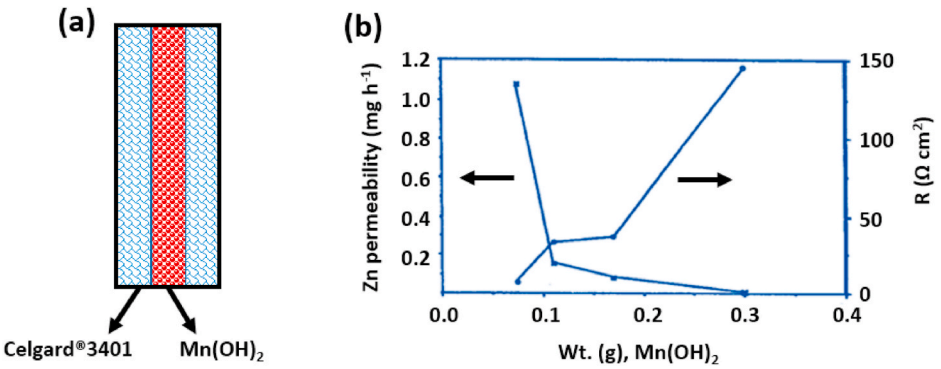

Fig. 4. Schematic representation of a composite membrane (a) and Zn permeability and resistance as a function of amount of $Mn(OH)_2$ (g) coated on the Celgard® 3401 (b). Fig. 3b is adapted with permission from Ref. [156]. Copyright Elsevier 1996.

On the other hand, despite the potential role of nanoparticle-filled composite membranes in minimizing the crossover of $Zn(OH)_4^{2-}$ ions, few studies are reported in the literature. ZIRFON® PERL (Agfa Specialty Products) membrane (pore size of 130 nm) that consists of a polysulfone network and zirconium oxide [182–184] has been used in Zn-air flow battery [185]. The ZIRFON® PERL-based battery exhibited above 50% round trip efficiency and the performance was not altered after l00 h of cycling at 25 mA cm^{-2}. Kiros [156] modified Celgard® 3401 (50 nm pore size, electrical resistance of 0.1 Ω cm^2 at room temperature and in a 6 M KOH solution) using insoluble inorganic compounds, such as $Al(OH)_3$, CaF_2, $Mg(OH)_2$ and $Mn(OH)_2$. Since they possess a very low solubility, after gelation/precipitation, they were sandwich between two Celgard® 3401 membranes, as schematically shown in Fig. 4a. Coating the membrane with $Mn(OH)_2$ produced the highest $Zn(OH)_4^{2-}$ ion-separation capacity, with no crossover of Zn $(OH)_4^{2-}$ ions. Coating of the membrane (10 cm^2) with 0.3 g of $Mn(OH)_2$ almost completely blocked the $Zn(OH)_4^{2-}$ permeation (only 0.03 mg/h of $Zn(OH)_4^{2-}$ ions crossover occurred). On the other hand, the use of two Celgard® 3401 membranes together (Fig. 4a) resulted in $Zn(OH)_4^{2-}$ crossover of 28.46 mg h^{-1} (close to 1000 times higher).

Nevertheless, the ohmic resistance of the membrane was dramatically increased especially with a higher amount of $Mn(OH)_2$ coating due to the plugging of the pores of the membrane by the fine colloidal particles (Fig. 4b). The electrical resistance of the Celgard® 3401 increased from 0.1 to about 150 Ω cm^2 (factor of 1500) when 0.3 g of $Mn(OH)_2$ were coated on the membrane in a 6 M KOH solution at room temperature. This has a negative impact on the OH^- ion conductivity and, thus on the overall performance of the battery. Therefore, the coating of porous membranes with an optimized amount of insoluble particles without a significant increase in their resistance is required in order to

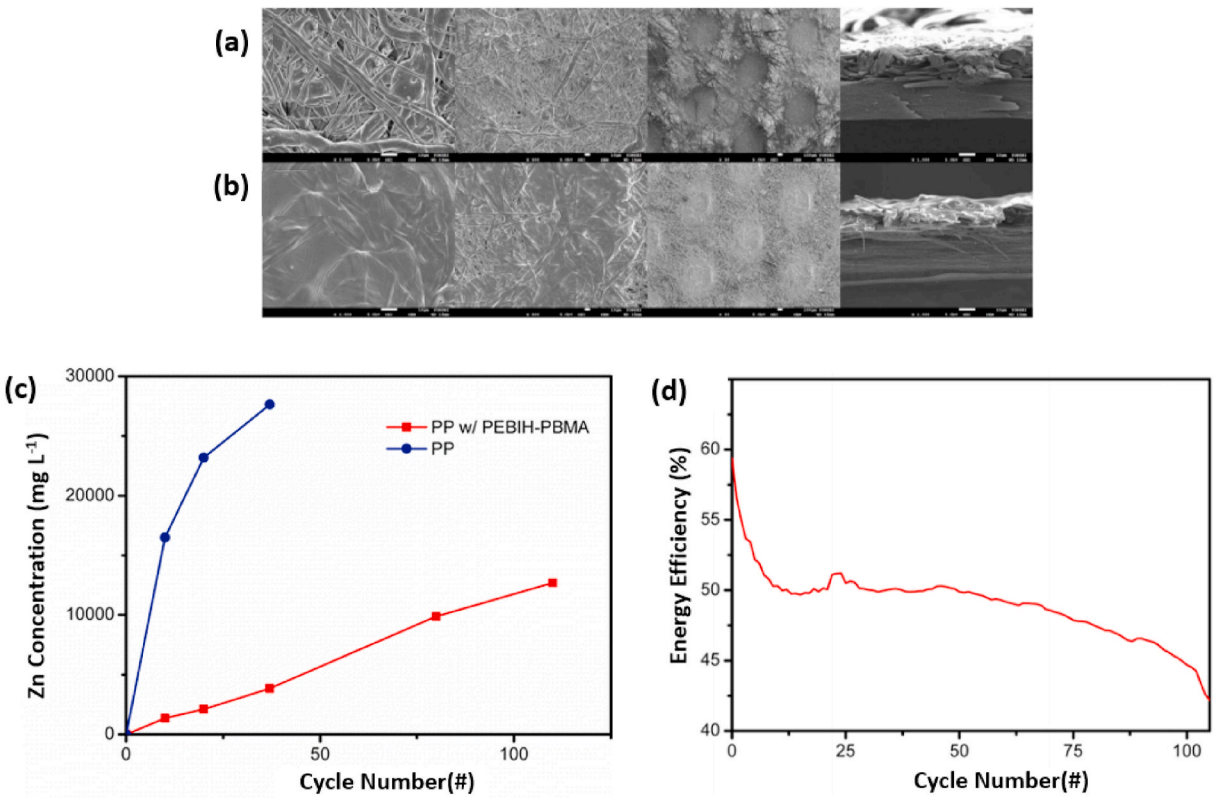

Fig. 5. SEM images of Celgard® 5550 (a) and Celgard® 5550 coated with PEBIH-PBMA (b), Zn concentration with cycle number (c) and Energy efficiency for Celgard® 5550 coated with PEBIH-PBMA under the constant current mode at 10 mA cm^{-2} (d). Reprinted with permission from Ref. [83]. Copyright © 2016 American Chemical Society.

justify their use in Zn-air batteries.

3.1.3.2. Coating porous membranes with ion-selective polymers. Another method to minimize the crossover of zincate ions is coating the porous membranes with an ion-selective layer. The coat is expected to allow OH^- transfer through the membrane and to minimize the migration of zincate ions to the cathode compartment without significantly affecting the ionic conductivity. Moreover, the porous part of the membrane can serve as a mechanical support and an additional barrier to the zincate ions passage based on their size exclusion effect. Various layer support options are available commercially, such as cellophane 350PØØ and Celgard® 5550 and 3501 etc.

On the other hand, there is still a need for developing alkaline stable, water-insoluble anionic-exchange polymers. Polymerized ionic liquids (PILs) are one promising class of candidates for tuning the membrane permselectivity to OH^-. Hwang et al. [83] coated a Celgard® 5550 membrane with PIL to prepare bilayer membranes for a rechargeable Zn-air battery. The anion exchange polymer (PEBIH-PBMA) coating layer was prepared via free radical polymerization, i.e., by copolymerization of two monomers: 1-[(4-ethenylphenyl) methyl] -3- butylimidazolium hydroxide (EBIH) and butyl methacrylate (BMA).

The surface and cross-sectional FE-SEM images of the Celgard® 5550 and PEBIH-PBMA coated Celgard® 5550 membranes are shown in Fig. 5a and Fig. 5b, respectively. However, no thickness increase is seen by the SEM images after coating compared to the original thickness of the Celgard® 5550 (25 μm), thus indicating a possible penetration of the viscous anionic-polymer solution onto the porous structure of the support layer despite the use of a highly viscous solution (20 wt % of polymer in ethanol). Over 96% reduction in the transport of $Zn(OH)_4^{2-}$ ions through the membrane to the cathode compartment was achieved. Compared to the Celgard® 5550 membrane, the modified membrane has over 2 magnitudes of $Zn(OH)_4^{2-}$ ions diffusion coefficient. Fig. 5c presents $Zn(OH)_4^{2-}$ concentration levels of the cathode electrolyte versus cycle number. The high selectivity is explained by the lower mobility $Zn(OH)_4^{2-}$ ion associated with their size exclusion. This was reported to enhance the durability of the battery as its life-span was increased by about 300% compared to the same battery using a non-modified membrane (37 vs 104 cycles).

Besides this three-fold improvement in lifetime of the battery, the modified membrane-based battery exhibited comparable initial energy efficiency with the Celgard® 5550-based one (60.8 vs 59.4%). On the other hand, the Celgard® 5550-based battery displayed higher final energy efficiency than the coated-ones (51.2 vs 41.8%), suggesting that the Celgard® 5550-based battery has prematurely deceased due to the $Zn(OH)_4^{2-}$ ions rather than degradation of the air-electrode catalyst. The modified membrane displayed a similar overpotential increase during both the discharge and charge steps, whereas, the Celgard® 5550 membrane did not. The ORR characteristics was found to remain unchanged, whereas the OER process exhibited difficulties manifested as overpotential growth, which resulted in a higher final voltage. The OER catalyst is expected to be more sensitive toward $Zn(OH)_4^{2-}$ exposure. The energy efficiency plot of PEBIH-PBMA coated membrane is presented in Fig. 5d.

Nafion® 117 (CEM) has been reported to improve the selectivity of Celgard® 3401 and Celgard® 3501 membranes [135]. Celgard® membranes are usually hydrophilized by treatment with a (cationic/nonionic) surfactant. In this work, to prepare hydrophobic membranes, the surfactant was removed by washing it out several times with methanol. The Celgard® membranes (with and without surfactant) were coated with a solution of Nafion® 117 (from its alcoholic or aqueous dispersions of various concentrations) using several techniques. When the Celgard® 3401 without surfactant was coated with a 1% Nafion® solution, no zincate ion transport during 5 h was reported. However, a high resistance was obtained (186 Ω cm^2 at 50 kHz) due to the hydrophobization of the membrane. The hydrophobic pores of the membrane have probably excluded the Nafion® solution and remained filled with trapped air (rendering low conductivity). An increase in both conductivity and zincate ion flux through the membrane was observed when a membrane with surfactant was used (Table 4). Moreover, higher zincate crossover and ionic conductivity were observed with an increase in the amount of Nafion® coated on Celgard® 3501 without surfactant. For example, the zincate ion diffusion coefficient for the Celgard® 3501 coated with 0.047 mg cm^{-2} of Nafion® was 1.1 × 10^{-12} m^2 s^{-1}, and across the membrane with 0.079 mg cm^{-2} of Nafion®, it was much higher: 8.3 × 10^{-12} m^2 s^{-1}. Based on this study, coating with Nafion® seems to be not efficient method to improve permselectivity of the membranes.

3.1.3.3. Sulfonated porous membranes. A limitation associated with the use of some commercial porous membranes is their hydrophobicity, which could decrease the pore wettability with KOH aqueous solution. A common strategy to enhance the hydrophilicity is by membrane surface modification. Sulfonation is a unique chemical treatment that can increase polymer hydrophilicity by incorporating sulfonic acid functional group on the surface of polymer [186]. Wu et al. [187] prepared sulfonated membranes with a high ionic conductivity and evaluated their

Table 4
Zincate crossover through pristine and modified porous membranes.

Membrane		Analysis method	Flux of $Zn(OH)_4^{2-}$ (× 10^{-6} mol m^{-2} s^{-1})	Diffusion coefficient of Zn $(OH)_4^{2-}$ (m^2 s^{-1})[c]	Ref.
Two Celgard® 3401		Electrogravimetric	120.8	6.9 × 10^{-12}	[156]
Two Celgard® 3401 coated with inorganic molecules	$Al(OH)_2$ + Teflon		21.2	8.5 × 10^{-12}	
	CaF_2		15.6	1.8 × 10^{-12}	
	$Mg(OH)_2$		0.31	5.1 × 10^{-14}	
	$Mn(OH)_2$		0.14	6.0 × 10^{-15}	
Celgard® 5550		ICP-OES	–	1.1 × 10^{-5}	[83]
Celgard® 5550 coated with PIL (PEBIH−PBMA)			–	5.0 × 10^{-7}	
Celgard® 3501 with surfactant (hydrophilic)		Polarography measurement	94.4	2.4 × 10^{-11}	[135]
Celgard® 3501 without surfactant (hydrophobic)			0[b]	0	
Celgard® 3501 coated with Nafion® 117[a]	0.024 mg cm^{-2} Nafion® 117		1	2.5 × 10^{-13}	
	0.047 mg cm^{-2} Nafion® 117		4.4	1.1 × 10^{-12}	
	0.079 mg cm^{-2} Nafion® 117		33.3	8.3 × 10^{-12}	
Celgard® 3401 coated with Coated with 1% Nafion® 117[a]	Without surfactant		0	0	
	With surfactant		45.6	5.8 × 10^{-13}	
Electrospun nanofiber membrane	Electrospun nanofibre mat-reinforced composite polymer (ERC) membranes	ICP-OES	–	8.33 × 10^{-12}	[85]
Inorganic membrane	NaSICON membrane	ASV analysis	–	8.5 × 10^{-15}	[134]

[a] Diffusion coefficient calculated (using Fick's law) based on the provided flux data.
[b] Not detected during the first 5 h of operation.
[c] Diffusion coefficient of $Zn(OH)_4^{2-}$ performed at room temperature.

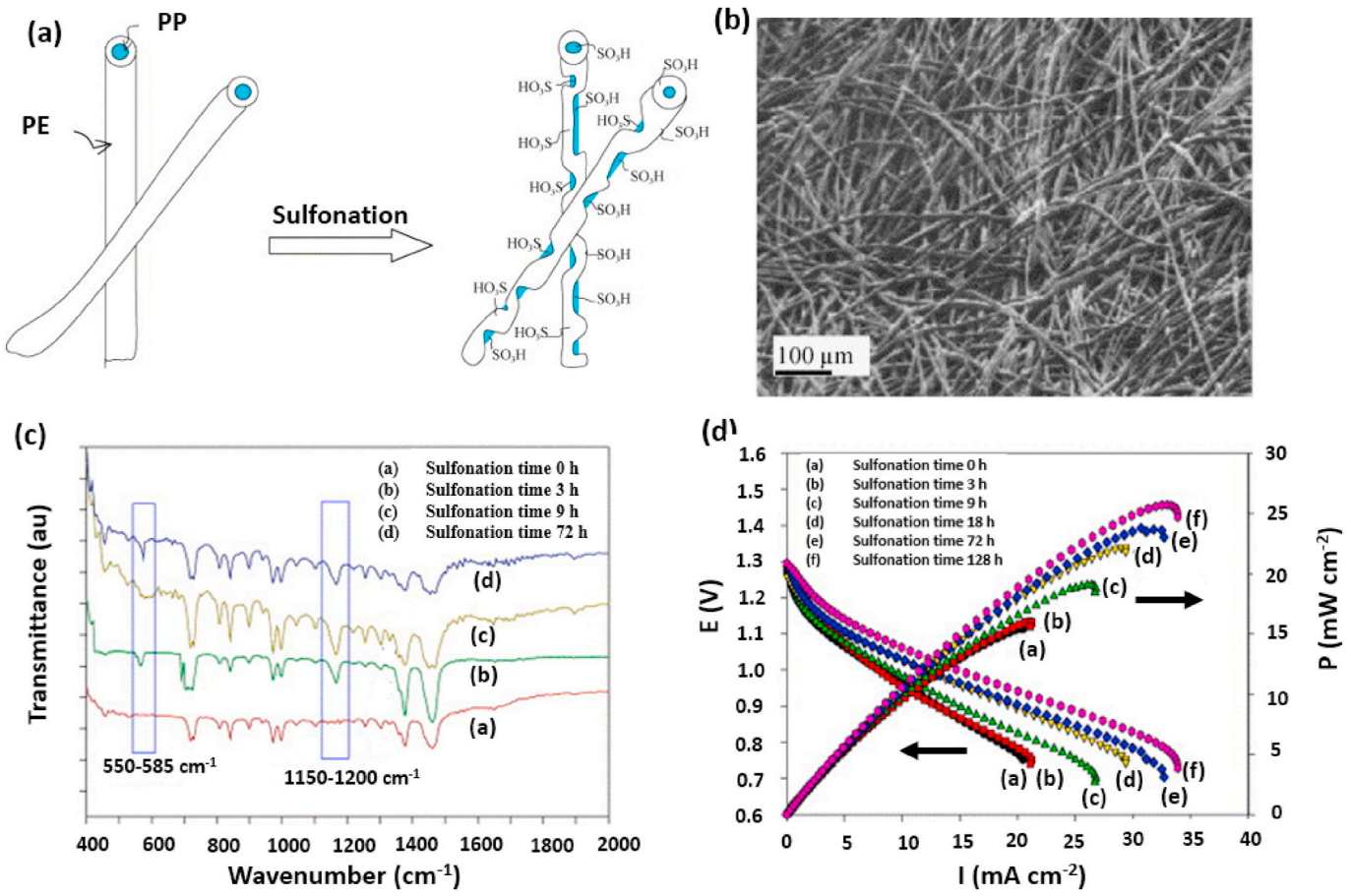

Fig. 6. Schematic illustrations of the non-woven membrane structures before and after the sulfonation treatment (a), SEM micrographs of the sulfonated s-PP/PE membrane (sulfonation time 128 h) (b), IR spectra of the different membrane samples (c) and the cell potential and power density curves of the solid-state zinc-air batteries as functions of discharge current density (d). Adapted with permission from Ref. [187]. Copyright © 2006 Elsevier.

performance in a Zn-air battery. These membranes were prepared by sulfonation of commercial non-woven PP/PE membranes (thickness = 0.2 mm, porosity = 60–70%) using concentrated sulfuric acid (Fig. 6a). The sulfonation reaction took place by immersing the PP/PE membranes in a 98 wt% sulfuric acid at 90 °C and atmospheric pressure for 3–128 h. The highly sulfonated s-PP/PE membrane (sulfonation time 128 h) is shown in Fig. 6b. As shown by the infrared spectra of the membranes (before and after the sulfonation treatment) in Fig. 6c, the peaks at around the wavenumbers of 1150–1200 and 550–585 cm^{-1} can be attributed to the asymmetric SO_3^- stretching modes and deformation of the S–O bonds, respectively, showing successful incorporation of sulfonic acid groups to the polymer membrane. However, after sulfonation, many of the filaments (originally, 10–20 μm) showed a reduced diameter indicating that part of the polymer had been degraded or/and dissolved by the sulfuric acid.

The water contact angles decreased from 58° (commercial PP/PE membrane) to 18° after 128 h of sulfonation, showing the effectiveness of the sulfonation in increasing surface hydrophilicity. The sulfonated membrane exhibited a higher ionic conductivity than that of the unsulfonated being 17.5 mS cm^{-1} vs 8.8 mS cm^{-1} at 25 °C (32 wt% KOH solution) and, thus, a higher power density of 38 mW cm^{-2} vs 20 mW cm^{-2} (Fig. 6d). However, compared to the pristine membrane, the sulfonated membrane showed a decrease in both tensile strength (21%) and thermal resistance (4%). The decrease in mechanical strength can be attributed to the surface etching effect of sulfuric acid, leading to decrease filaments diameter and, probably lower polymer molecular weight.

3.1.4. Inorganic membranes

Inorganic membranes refer to membranes which are made from materials such as ceramic, magnesia, alumina and titania. Inorganic membranes are known for their high chemical and thermal stability. These membranes are interesting as potential candidates for Zn-air batteries because of their good alkaline chemical stability [188]. Additionally, hydrotalcite clay is an interesting alkaline AEM material [189], but has never been exploited for Zn-air batteries. A ceramic membrane could provide the required dimensional rigidity that could be effective in avoiding internal short circuit problem. Moreover, ceramic membranes are known to have better chemical stability (against oxidative agents) compared to polymeric membranes [190,191]. However, despite the excellent alkaline stability, almost no attention has been given to the preparation of such membranes for Zn-air flow batteries. This could be due to the fact that inorganic porous membranes are usually fragile [192,193]. Therefore, it is difficult and expensive to fabricate large inorganic membranes [87].

Ceramic membranes which are impermeable to $Zn(OH)_4^{2-}$ has been evaluated in rechargeable alkaline Zn/MnO_2 batteries [134]. In this study, a commercial sodium super-ion conducting ceramic membrane (NaSICON) was used. Here, the Na^+ cation is the charge carrier, rather than the OH^- ion. Due to its inherent property (cation conductor) and solid-state nature of the membrane, no $Zn(OH)_4^{2-}$ crossover was detected. Nevertheless, the membrane (1.17 cm^2) had high resistance values: 26 Ω for the 1.0 mm thick and 11 Ω for the 0.5 mm thick NaSICON membrane, strongly suggesting that a decrease in membrane thickness is required. However, such strategy will probably result in a brittle membrane.

Saputra et al. [172] prepared microporous MCM-41 membrane by a facile, dip-coating technique from a solution consisting of cethyltrimethylammonium bromide (CTAB), hydrochloric acid, DI water, ethanol and tetraethylorthosilicate (TEOS). MCM-41 membrane (thickness ca. 5 μm and average pore size 2.2 nm) with hexagonally ordered, narrow, pore structure formation was verified using X-ray diffraction. The membranes tested in Zn/MCM-41/air cell using KOH electrolyte displaying a good performance: a maximum power density of 32 mW cm^{-2} and energy density of 300 Wh L^{-1}, which was comparable to that of commercial Zn-air button cells of equivalent size was reported.

Table 4 presents the diffusion coefficients of $Zn(OH)_4^{2-}$ ions through the pristine and porous polymeric membranes. The porous Celgard® membranes are included in the table for comparison purpose.

3.2. Polymer electrolyte membranes (ion-conducting membranes)

3.2.1. Anion-exchange membranes

An AEM consists of polymer chains functionalized with a number of cationic groups. Most AEMs are made from hydrocarbon polymer backbones with covalently attached quaternary ammonium (QA) groups. The use of AEMs in Zn-air batteries have been widely proposed [65] since a typical AEM exhibit only a 10% loss in performance after 1000 h [44]. This performance is more than satisfactory for meeting the required shelf life and cycle life of the battery. However, no information has been provided regarding the AEM type and battery testing conditions. The prospects for AEMs in Zn-air batteries, including the major recent developments and strategies to overcome the remaining challenges has been reviewed recently [194]. Indeed, the performance and cyclability of the batteries have been found to be dependent on the properties of the AEMs (such as water uptake, anisotropic swelling ratio and hydroxide conductivity). Additionally, the common AEMs chemical degradation ways and their mitigation strategies have been discussed.

A commercial AEM A201® (Tokuyama Soda, Japan) has been tested in Zn-air batteries. The A201®-based battery showed a rapid voltage and capacity loss after some cycles. This was attributed to the continuous loss of membrane water content and ionic conductivity during the constant current operation [142–145]. To solve this issue, AEMs following different synthesis strategies have been prepared and tested in Zn-air batteries [142–145]. The prepared AEMs which exhibit superior OH^- ion conductive properties, water retention and low anisotropic swelling were reported to boost the specific capacity and improved the cycling stability of the battery compared to that of A201®-based battery (Table 5). However, the effect of zincate ions crossover was not investigated in these studies.

Dewi et al. [84] synthesized AEM by using polysulfonium cation (poly(methylsulfo-nio-1,4-phenylenethio-1,4-phenylene trifluoromethanesul-fonate). The prepared polysulfonium-based membrane was effective in preventing zincate ions crossover from the negative to the positive electrode, leading to a more than 6-fold discharge capacity increase of the cell compared to the case of using a Celgard® 5550 membrane. It was assumed that Zn (II) species in the electrolyte are able to cross through the membrane to the air electrode in the form of Zn^{2+}. However, in a strongly alkaline solution, the Zn^{2+} ions combine with OH^- ions, instantly forming $Zn(OH)_4^{2-}$ ions.

Fu et al. [142] prepared a flexible, highly conductive (21 mS cm^{-1} at 30 °C) nanoporous membrane from natural cellulose nanofibers with very high water retention (96.5%) and low anisotropic swelling degree (1.1). The membrane was prepared via functionalization of the cellulose fibers using dimethyloctadecyl[3-(trimethoxysilyl)propyl] ammonium chloride (DMOAP) (in methanol) as a precursor. The mixture of DMOAP and cellulose fibers was stirred (12 h at room temperature), centrifuged and washed (with ethanol and distilled deionized water) to remove unreacted traces of DMOAP. The QA-functionalized cellulose (QAFC) membrane was prepared by vacuum filtration, followed by drying and crosslinking. The reference A201® membrane exhibited an anisotropic swelling degree of 4.4 and water uptake of 44.3%. As a result, the 2-QAFC (cellulose nanofibers modified with 200 mol. % concentration of DMOAP with respect to the cellulose repeating glucose unit) membrane-based battery was reported to have a higher discharge capacity with a more stable voltage compared to the A201®-based battery.

Zhang et al. [143] prepared a laminated, cross-linked nanocellulose/graphene oxide membrane functionalized with QA for a flexible rechargeable Zn-air battery. Here, Graphene oxide (GO) was incorporated in order to enhance the ionic conductivity since it has abundant oxygen-containing groups which can be easily functionalized. Cellulose fibers are used as interconnected framework to integrate GO into a flexible membrane with a high water content, which can be cross-linked to achieve the required structural stability and (low) anisotropic swelling degree. Fig. 7a shows the procedure followed for the preparation of the 2-QAFGO membrane. The QA-functionalized nanocellulose/GO (QAFCGO) membrane showed superior OH^- conductivity of 33 mS cm^{-1} at room temperature. The QAFCGO-based battery was reported to show higher performance compared to the A201®-based battery, with smaller over potentials for both discharge and charge processes. At current densities above 20 mA cm^{-2}, the QAFCGO-based battery remarkably outperformed the A201®-based battery (Fig. 7b). The former battery had a better cycling stability performance than the latter one (Fig. 7c). Moreover, the QAFCGO-based battery reached a higher peak power density (44 mW cm^{-2}) than the A201®-based one (33 mW cm^{-2}) (Fig. 7d).

Furthermore, Abbasi et al. [155] prepared three AEMs using poly (p-phenylene oxide) (PPO) as polymer backbone and three different cations - trimethylamine (TMA), 1-methylpyrolidine (MPY), and 1-methylimidazole (MIM). PPO was chosen as a polymer backbone due to its commercial availability, high thermal, mechanical, and acceptable chemical stability and facile postfunctionalization [195,196]. The cations were directly attached on the PPO backbone. The PPO-TMA membrane was reported to have OH^- ion conductivity equal to 17 mS cm^{-1}, 89 wt% water uptake at room temperature and to prevent the crossover of $Zn(OH)_4^{2-}$ ions (Table 6). Moreover, the membrane showed excellent alkaline stability for at least 150 h in an alkaline solution commonly used in Zn–air batteries (7 M KOH solution at 30 °C). The PPO-TMA–based Zn-air battery exhibited low zincate diffusion coefficients (1.9×10^{-14} m^2 s^{-1}) and high specific discharge capacity (~800 mAh g_{Zn}^{-1}). The low zincate diffusion coefficient of the PPO-based membrane was ascribed to the formation of ionic channels in the polymer structure through hydrophilic/hydrophobic microphase separation. However, no experimental evidence was provided for the formation of such a hydrophilic/hydrophobic microphase separation structure.

Well-defined hydrophilic-hydrophobic phase separation is crucial for enhancing ionic conductivity of AEMs [197]. However, not all AEMs develop a phase separation structure. Different strategies, such as block copolymers [198] and cation functionalization via a long-spacer-chain [199] have been used to design an AEM with a phase separation structure. AEMs composed of PVA/guar hydroxypropyltrimonium chloride (PGG-GP) displaying a hydrophilic-hydrophobic microphase separation structure and large ionic clusters was developed by using GA and pyrrole-2-carboxaldehyde as binary cross-linking agents. The prepared PGG-GP membrane exhibited a high OH^- ion conductivity (123 mS cm^{-1} at room temperature) and an excellent dimensional stability. The PGG-GP-based, flexible, all-solid-state Zn–air battery displayed a peak power density of 50.2 mW cm^{-2} at 48 mA cm^{-2} and a promising cycling stability (9 h at 2 mA cm^{-2}) [121]. On the other hand, formation of ionic channels with appropriate sizes in the two domains is required to develop AEMs with high selectivity [194].

Recently, an interesting investigation of effect of microdomain morphology on selective $Zn(OH)_4^{2-}$ and OH^- ions transport was performed [200]. PILs-based liquid-crystalline AEM with inverse bicontinuous cubic ($Ia\bar{3}d$) structure was prepared through a one-step chemical synthesis. The AEM-$Ia\bar{3}d$, with IEC of 0.76 mmol/g, had an OH^- conductivity of 12.6 mS cm^{-1} at 30 °C. Whereas, the crossover of hydrated

Table 5
Anion exchange membranes used in Zn-air batteries.

Membrane type	Preparation method	Properties	Battery type and operation conditions	Electrodes	Electrolyte	Performance	Ref.
FAA®-3-based AEM	Commercial FAA®-3-SOLUT-10 in NMP, Fumatech BWT GmbH) Solution casting method.	QA cation	Bendable rechargeable Zn–air battery	Zn electrode: stainless-steel mesh coat with Zn species Air electrode: cobalt oxide based commercial	6 mol KOH PAA gel	Maximum power density of 9.8 mW cm^{-2}. Cells stable for at least 100 cycles. Specific capacity ~700 mAh g_{Zn}^{-1} under 1 mA cm^{-2} and discharging conditions.	[201]
A201® membrane	Commercial (Tokuyama Corporation, Japan)	28 μm thickness	Solid state rechargeable Zn-air battery	Zn electrode: Zn powder, carbon nanofiber, carbon black and poly (vinylidene fluoride-co -hexafluoropropene) polymer binder. Air electrode: Co_3O_4 nano-particles (<50 nm particle size) Gas diffusion layer: (catalyst loading of 1.0 mg cm^{-2})	–	A201-based battery membrane deteriorated noticeably after 720 min - The rapid voltage and capacity loss due to water loss	[142]
Polysulfonium-based membrane	Solution casting method	Transparent, 30 μm thickness	Zn-air cell, The cells were discharged at 1 mA at room temperature	Zn electrode: Zn powder (99.9% grade) (1 g) Air electrode: Carbon paste that contained MnO_2 catalyst	1 M KOH	Capacities of discharge cell: 0.6 V, 124.8 h, 86 mAh g_{Zn}^{-1}	[84]
PPO-based AEM	Solution casting method	uniform and flexible films, 50 μm thickness	Primary Zn-air battery effective membrane and electrode area of 1.77 cm^2 The cell was discharged at a constant discharge current in the range of 2.5–15 mA cm^{-2} All experiments, the cut-off voltage was 0.9 V.	Zn electrode: anode was a 1 × 1 cm^2 pure zinc plate Cathode electrode: Ni-foam used as the current collector and gas diffusion layer. Mixture of MnO_2 and VXC-72 was used to prepare catalyst.	7 M KOH solution	PPO–MPY based cells: -maximum discharge current density of 117 mA/cm^2 with a maximum power density of 70 mW cm^{-2}. -Specific capacity: 772 mAh g_{Zn}^{-1} at 2.5 mA cm^{-2} -Power of the cell was 996 mWh g_{Zn}^{-1} for 2.5 mA cm^{-2} discharge current density.	[155]
Porous AEM based on QA and nanocellulose	Functionalization, followed by crosslinking.	High flexible, thickness of 30 μm	Solid state rechargeable Zn-air battery	Zn electrode (40 mg): Zn powder, carbon nanofiber, carbon black and poly (vinylidene fluoride-co -hexafluoropropene) polymer binder. Air electrode: Co_3O_4 nano-particles (<50 nm particle size) Gas diffusion layer: (catalyst loading of 1.0 mg/cm^2) Catalyst ink consisted of Co_3O_4, ionomer (AS-4, Tokuyama Inc.) and 1-propanol was sprayed onto a carbon cloth	–	2-QAFC battery - Specific capacity of was 492 mA h g_{Zn}^{-1}. - High power density of 2362 mW g_{Zn}^{-1} at a large current density of 4650 mA g_{Zn}^{-1} -Cycling stability over 2100 min.	[142]
Laminated cross-linked nanocellulose/GO	Vacuum filtration, followed by cross-linking	Thickness = 30–50 μm	Flexible rechargeable Zn–air battery	Zn electrode: Zn film (zinc powder, carbon nanofiber, carbon black, and poly (vinylidene fluoride-co-hexafluoropropene) polymer binder) Air electrode: Co_3O_4 nanoparticles (<50 nm particle size) spayed onto a carbon cloth	–	QAFCGO-based battery: -Power density 44 mW cm^{-2}. -Stable output power within current density of 60 mA cm^{-2} under stressed conditions	[143]
GO membrane functionalized with imidazolium (1-hexyl-3-	Solution casting/ vacuum filtration method	27 μm thickness,	Fully solid-state, thin, flexible Zn–air battery	Zn pellet electrode Gas-diffusion layer: active material and carbon black in	–	The 5-HMIM/G (5 = HMIM/GO)-battery:	[144]

(continued on next page)

Table 5 (*continued*)

Membrane type	Preparation method	Properties	Battery type and operation conditions	Electrodes	Electrolyte	Performance	Ref.
methylimidazolium chloride, HMIM)		flexible and tough	active surface area of 1.13 cm^2	isopropyl alcohol with binder (AS-4 ionomer, Tokuyama Inc.) A bifunctional Co_3O_4 Loading of the active material on the air electrode was 1.0 mg cm^{-2}		-Stable charge/ discharge performance for 60 cycles -Specific energy density dropped only 16.6 Wh kg_{zn}^{-1} as the specific power density increase from 120 to 360 W kg_{zn}^{-1}	
Cross-linked chitosan (CS) and poly (diallyldimethylammonium chloride) (PDDA)	Solution casting method	Anisotropic swelling (1.7) degree and water uptake (1.59 g g^{-1})	Solid-state Zn–air battery	Zn electrode: Zn metal Air electrode: 20 wt% Pt/C and IrO_2 (Ir = 85.7%) Catalyst ink consisted of 40 mg catalyst, 80 μL of 5 wt% Nafion and 10 mL ethanol.	–	The CS-PDDA-based battery: -High open-circuit voltage (1.3 V) -High power density (48.9 mW cm^{-2}) at 100 mA cm^{-2} but a limited cycle life of 2.5 h.	[145]
AEM composed of PVA/guar hydroxypropyltrimonium chloride (PGG-GP)	Solution casting, followed by cross-linking	1.52 mequiv/g IEC, anisotropic swelling degree (1.5) Thickness: 30–40 μm	All-solid-state Zn–air battery	Zn electrode: polished Zn foil Air electrode: IrO_2 and 40 wt% Pt/C Catalyst ink consisted of IrO_2/Pt/C (1:1 by mass), 5 wt % Nafion and ethanol	–	-Peak power density of 50 mW cm^{-2} at 48 mA cm^{-2} -Cycling stability of 9 h at 2 mA cm^{-2}.	[121]

*It should be noted that the theoretical specific capacity of Zn is 820 mAh g_{Zn}^{-1}.

$Zn(OH)_4^{2-}$ was found to be hindered ($Zn(OH)_4^{2-}$ diffusion coefficient of 1.6×10^{-13} m^2 s^{-1}). This well-defined 3D-interconnected ionic channels and the size-exclusion effect played a role to enhance the OH^- permselectivity of the membrane.

3.2.2. Cation-exchange membranes

Nafion®, composed of a perfluorinated polymer backbone with pendant perfluoro ether terminated sulfonic acid side chains (PFSA), is the most frequently used material as a proton exchange membrane in fuel cells. It is chemically stable and has a high phase-separated morphology which makes it of possible interest for Zn-air battery applications. The water domains in PFSA membranes have been reported to be organized as locally flat and narrow (around 1 nm) channels [202]. This agrees with the finding of cryo-TEM tomographs of hydrated Nafion® membrane [203]. However, the hydrophilic negatively-charged sulfonate group in the Nafion® film allows the transportation of positively charged species while blocking negatively charged species, such as OH^- and $Zn(OH)_4^{2-}$ ions.

Therefore, when Nafion® is used in Zn-air battery, both $Zn(OH)_4^{2-}$ and OH^- ions will be repulsed by the Donnan exclusion mechanism; however, some OH^- ions (co-ions) can still permeate through the hydrophilic phase since the Nafion® membrane swelling is high in aqueous media [204] and especially in electrolyte solutions of the high ionic strength [205]. Indeed, the diffusion coefficient of $Zn(OH)_4^{2-}$ ion of Nafion® 521 film tested in a Zn-air battery was reported to be very low, 6.67×10^{-14} m^2 s^{-1} [86]. However, the Nafion® 521 film showed also a rather low OH^- transference number of 0.14 [86] since as expected the protons conductivity was favored resulting in extremely low (0.8 mS cm^{-1}) OH^- ion conductivity at room temperature. As a result, the Nafion® film-based Zn–air battery showed considerably large discharge/charge polarization, resulting in a very poor cyclic stability. Similarly, in another study, Nafion® 117-based Zn-air fuel cell was reported to exhibit a poor performance (0.4 V at 1.3 mA cm^{-2}) [79].

Overall, Nafion® membranes afford a low voltage efficiency, even at low working current densities, in batteries using alkaline electrolytes. Therefore, given its low performance and high cost, it can be concluded that Nafion® membranes are not suitable for alkaline electrolyte-based batteries [204].

On the other hand, since Nafion® film has negative fixed charged groups that prevent the passage of $Zn(OH)_4^{2-}$ ions, it can be used to improve the selectivity of the membranes in Zn-air batteries. For example, Kim et al. [86] fabricated polymer blend electrolyte membranes (PBE membranes) (24 μm thick) by impregnating Nafion® films into an electrospun PVA/PAA nanofiber mat for rechargeable Zn-air battery. The Nafion® acts as an anion-repelling continuous polymeric phase. This was reported to effectively block $Zn(OH)_4^{2-}$ ions crossover with only slightly reducing the OH^- conduction. As a result, the PBE membranes had better cyclic stability compared to Celgard® 3501 membrane (over 2500 min vs. 900 min).

A summary of zincate permeation through AEMs and CEMs is presented in Table 6. Porous membranes are also included in the table for the sake of comparison. Evidently, the reported $Zn(OH)_4^{2-}$ diffusion coefficients for AEMs are quite similar to that for the Nafion® 521 membrane. They were a much lower than those for the porous membranes and Nafion® bearing electrospun PVA/PAA mat (PBE membrane). For instance, the PPO-TMA membrane had a selectivity which is three order of magnitude higher than that of the Celgard® 3501 membrane. As stated in the previous section, this could be due to the formation of proper hydrophilic ions-conducting channels forming a hydrophilic-hydrophobic phase separation. The order of effectiveness in hindering zincate crossover of the membranes is: PPO–MPY > PPO–TMA > Nafion® 521 > AEM-Ia$\bar{3}$d > PBE > Celgard® 3501.

In most studies, only the observed decrease in zincate ions crossover is reported as an improvement. However, usually, this comes at the cost of a reduced OH^- ions conductivity. For instance, as shown in Table 6, Nafion® membrane has a quite low zincate ions crossover. Nevertheless, its OH^- conductivity was reported to be low as well. On the other hand, the AEMs displayed a low diffusion coefficient of $Zn(OH)_4^{2-}$ and high OH^- conductivity, showing their superior degree of selectivity. Therefore, a concept rarely used - permselectivity should be considered for comparing the membranes. The order of the membranes in terms of permselectivity is: PPO–MPY > PPO–TMA > AEM-Ia$\bar{3}$d > Nafion® 521 > PBE membrane > Celgard® 3501.

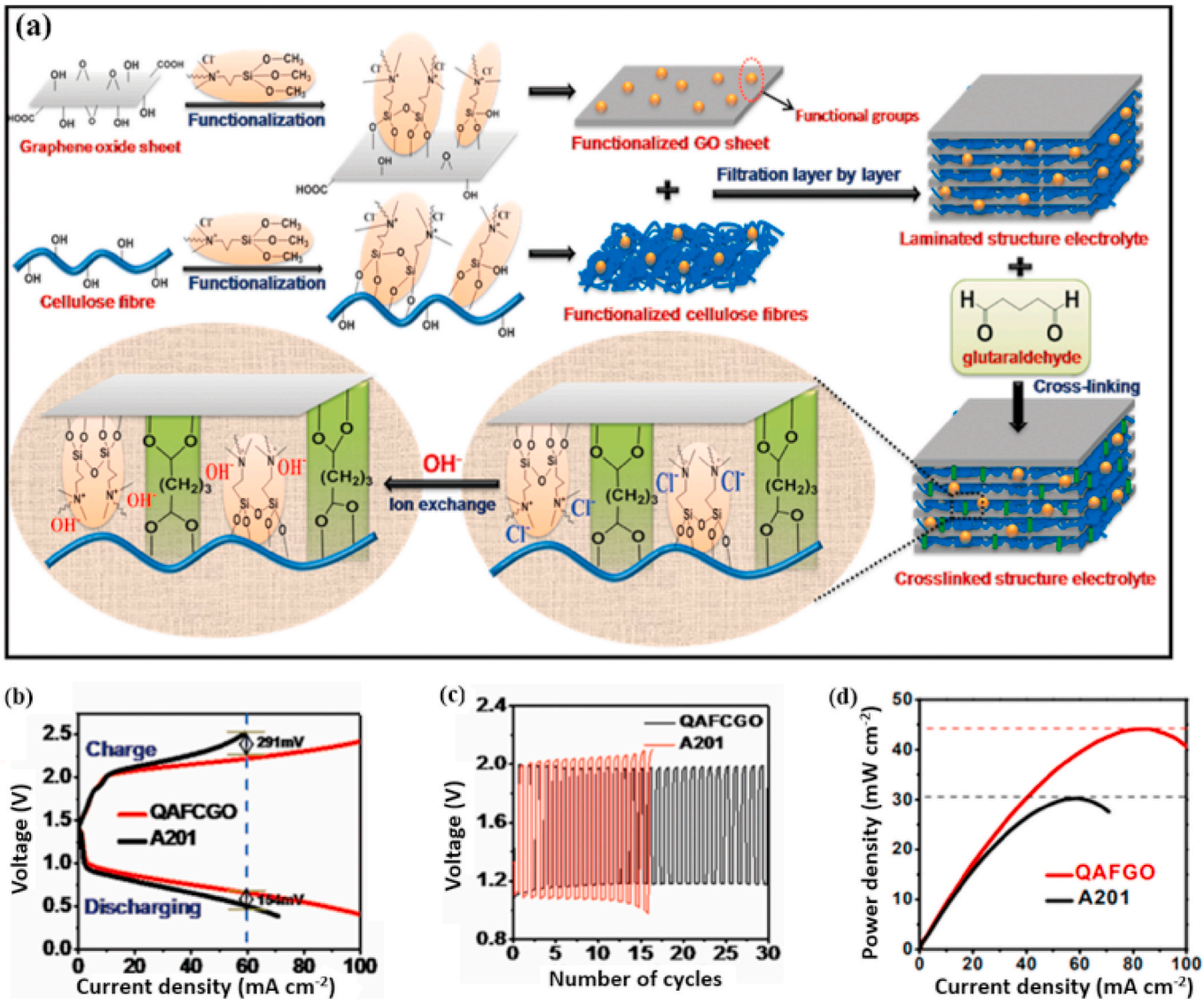

Fig. 7. QAFCGO and A201® membranes-based Zn-air batteries: Schematic diagram of the chemical structure evolution of the nanocellulose membrane by functionalization, cross-linking and hydroxide-exchange (a), charge and discharge polarization curves (b), galvanostatic charge and discharge cycling at a current density of 1 mA cm^{-2} with a 20 min per cycle period (10 min discharge followed by 10 min charge) (c) and the power density plots at a current density of 1 mA cm^{-2} (d). Reproduced with permission from Ref. [143]. Copyright 2016, Wiley-VCH.

Table 6
Zincate crossover through ion-conducting membranes.

Membrane		$Zn(OH)_4^{2-}$ diffusion coefficient (D) (m^2 s^{-1})	OH^- ions conductivity (σ) in water (mS cm^{-1}) (at room temperature)	Permselectivity (σ/D) (S.s m^{-3})	Ref.
AEM	PPO–TMA	1.9×10^{-14}	17.4	9.2×10^{13}	[155]
	PPO–MPY	4.7×10^{-15}	16.3	3.5×10^{14}	
	AEM-Ia$\bar{3}$d	1.6×10^{-13}	12.6	7.9×10^{12}	[200]
CEM	Nafion® 521 film	6.7×10^{-14}	0.8	1.2×10^{12}	[86]
	Nafion® bearing electrospun PVA/PAA mat (PBE)	6.8×10^{-13}	6.6	9.7×10^{11}	[85]
Porous (reference)	Celgard® 3501	3.20×10^{-11}	13.7	4.3×10^{10}	

It is worth noting that the comparison is dependent of the zincate ion crossover testing conditions and measurement techniques. For instance, the electrolyte used has been reported to have an effect on the degree of crossover. For the same membrane, a higher zincate diffusion coefficient was reported when KOH was used instead of NaOH. This was attributed to the larger conductivity of (35 wt%) KOH (620 mS cm^{-1}) [98] over (30 wt%) NaOH (190 mS cm^{-1}) [206]. Therefore, it is difficult to compare the membranes performance when the same electrolyte is not used. This requires further investigation for developing reliable standard membrane performance protocols.

Last but not least, it is worth identifying the zincate concentration at which a detrimental effect is seen in the air electrode activity and cell capacity. For example, in alkaline Zn/MnO_2 batteries, detrimental effects of $Zn(OH)_4^{2-}$ ions on the positive electrode have been reported to occur at concentrations $\geq$ 0.1 M $Zn(OH)_4^{2-}$ [207]. Besides, a study correlating AEM properties (mainly ion exchange capacity, nanochannel size and degree of zincate ions crossover) with cell performance and cyclic stability is missing.

3.2.3. Ion solvating membranes (gel-polymer electrolyte membranes)

Ion solvating membranes (gel-polymer electrolyte membranes) are usually used as membrane. Conventional aqueous electrolytes cannot maintain a steady form and, thus cannot effectively separate the electrodes to prevent a short circuit [208]. On the other hand, gel polymer electrolytes, composed of one or more polymers gelled by an aqueous electrolyte, have been widely employed in flexible Zn-based batteries as a membrane [209]. Ion solvating membranes rely on the aqueous alkaline electrolyte (typically, KOH) to provide their ionic conductivity and when swelled with the KOH, they tend to form a homogenous ternary polymer/water/KOH system [210]. The performance of these membranes greatly depends on the choice of polymer matrix and the proportion of each ingredient. Usually, vinyl polymers and cellulose derivatives are used as matrices since they swell well upon exposure to an alkaline aqueous solution [63].

Mostly, composite polymeric membranes with high swelling degree are used in Zn-air batteries. For instance, a cross-linked PAA/PVA gel polymer electrolyte (thickness = 28 μm) was prepared by thermal crosslinking (heat treatment: 140 °C for 3 h) method and used in a Zn-air cell [211]. The crossover of $Zn(OH)_4^{2-}$ ions through the crosslinked PVA/PAA (about 0.1 mmol) was significantly reduced compared with that of the Celgard® 3501 membrane (0.25 mmol) within 35 h of operation. More recently, Kim et al. [86] also prepared cross-linked PVA/PAA gel polymer electrolyte membrane (thickness, 24 μm) via thermal treatment of PVA and PAA mixture. Compared to the Zn-air cell with celgard® 3501 membrane, the cell with the PVA/PAA electrolyte membrane showed a better OH^- permselectivity and electrochemical properties. The membrane was effective (lowered by about a half), the $Zn(OH)_4^{2-}$ ions crossover compared to that of the celgard® 3501 membrane.

Yang et al. [212] reported the synthesis of a PVA-based gel polymer electrolyte that was doped with KOH. The PVA/KOH/H_2O electrolyte membrane exhibited a high ionic conductivity (47 mS cm^{-1} at room temperature) and good electrochemical performance. They also measured the anionic transport number (t^-) for PVA, PVA/PECH, and PVA/tetraethyl ammonium chloride (TEAC) polymer electrolytes using the Hittorf's method at 25 °C. The t^- (varying between 0.82 and 0.99) was found to be dependent on the types of alkali metal salts and the chemical compositions of polymer electrolytes [213]. The PVA/TEAC (PVA: TEAC = 1:1) blend membranes displayed an ionic conductivity of 23 mS cm^{-1} at room temperature.

A porous PVA-gelled polymer electrolyte prepared by a phase inversion method was used in rechargeable Zn–air battery [214]. After the phase inversion, the PVA membrane was cross-linked using a solution of 10 wt% glutaraldehyde (GA) in acetone at 30 °C for 10 min and immersed in a solution of KOH/PVA (35/2 wt%) for 24 h. The battery employing the PVA-gelled electrolyte membrane (20–50 μm) and highly flexible electrodes exhibited an excellent cycle stability over 120 cycles (at a volumetric charge-discharge rate of 250 A L^{-1}). The battery also demonstrated high volumetric (2905 Wh L^{-1}) and gravimetric (581 Wh kg^{-1}) energy densities. Furthermore, Peng et al. [215] reported a flexible, stretchable and rechargeable Zn-air battery using a PVA/poly (ethylene oxide) (PEO)–based alkaline polymer electrolyte. The discharge current density reached 1 A g^{-1} maintained for 30 discharge/charge cycles at a voltage plateau of 1.0 V. The influence of various properties of gel polymer electrolyte membranes, such as ionic conductivities, chemical stability, electrochemical windows and mechanical properties on the performance of rechargeable Zn–air batteries have been investigated elsewhere [216]. An inverse relationship between ionic conductivity and mechanical stiffness of the gel-polymer electrolytes was noticed. PAA6M-based battery exhibited the highest initial charge-discharge efficiency of 79% at 0.5 mA cm^{-2}. The performance was reported to be enhanced by reducing the gel polymer electrolyte thickness.

Modified gel-polymer electrolyte membranes have been also tested in Zn-air batteries. PEO-PVA-glass-fiber-mat (thickness controlled between 0.30 and 0.60 mm) with a high ionic conductivity (10 mS cm^{-1}) at room temperature has been prepared and employed in solid-state primary Zn–air cells by Yang and Lin [217]. The PEO–PVA polymer electrolyte showed a broad electrochemical stability window of 2.4 V (±1.2 V) [217]. The PEO–PVA-based Zn-air cell displayed a 1305 mA h capacity, thus with utilization of Zn 84% (since the theoretical capacity is 1560 mA h) at the C/10 rate at room temperature. On the other hand, the cell based on PE/PP's utilization was only 75%. The higher capacity and utilization of the cell employing the modified gel-polymer electrolyte membrane were attributed to its much smaller (0.1–0.2 μm) pores size compared with that of a PE/PP membrane (about 10–20 μm). On the other hand, the cell based on the PE/PP membrane was reported to be easily short-circuited when it is under a high discharge rate due to its larger pore size and non-uniform pore size distribution. Similarly, a gel polymer electrolyte consists of porous PVA and silica has been tested in Zn-air battery [218]. It was reported to show a high ionic conductivity (57 mS cm^{-1}) and a superior electrolyte retention capability out-performing that of the conventional PVA-KOH gel polymer electrolyte system.

4. Zn-dendrites growth suppressing membranes

One of the main challenges related to the presence of the Zn-electrode of rechargeable Zn-air batteries is the formation of Zn-dendrites [219]. During the reduction of ZnO to Zn metal, the $Zn(OH)_4^{2-}$ ions close to the Zn electrode surface are first depleted and most of the remaining are retained by the membrane (inside and/or its surface) or at the exterior of the electrolyte, thus resulting in an uneven distribution of $Zn(OH)_4^{2-}$ ions (severe concentration polarization) [80]. Zn-dendrites are formed as a result of the inhomogeneities in the electrode surface morphology and the electric field strength distribution across the Zn electrode, caused by the free diffusion of Zn ions in the vicinity of the electrode surface [80,220,221]. In other words, the diffusion-controlled Zn deposition process is influenced by both electric field and concentration gradients [222] and the inhomogeneity on the electrode surface brings about its formation since there is faster mass transport due to a non-planar Zn ions diffusion. Moreover, Zn-dendrites tend to develop at high current densities, which lead to a rapid Zn deposition, due to the resulting non-uniform concentration gradients [223]. This is similar to the dendritic growth mechanism model proposed for copper and lithium metallic electrodes [224–226].

The usually sharp-structured dendrites can puncture the membrane [227], especially when the amount of dendrites is increased. This can lead to an electrical short-circuit of the cell during the charging process and result in battery failure [227]. Therefore, reinforcement of the membranes is necessary in addition to the efforts to avoid the formation of dendrites.

To reduce/avoid the continuous formation and growth of Zn-dendrites, thus extending the battery life-span as much as possible, several strategies including addition of additives into electrolytes [228] and electrodes [229], modification of Zn-electrode structure [230], optimization of electrolyte properties and selection of appropriate membranes [168,231,232] have been so far employed. However, despite the important role of membranes in retarding Zn-dendrite formation, there are only few reported studies focusing on their effects [231,233].

The use of an ion-conductive and/or optimized porous membrane is

believed to improve the cycling stability of the battery by suppressing dendrite formations [234,235]. This is due to the fact that (i) membrane can regulate ion transport and avoid ion concentration gradient, which is the main cause of dendrite growth and (ii) the nanochannels in the membranes can greatly enhance the uniformity of current distribution resulting in a uniform Zn deposition [231]. For instance, prevention of Zn-dendrites formation has been observed when a membrane with a proper pore size and pore size distribution was used [168]. In this work, the microstructures of PVA/PVC membrane with pore size in the range of 60–120 nm were reported to effectively prevent any Zn dendritic formation during the overcharge period. As a result, over 50 cycles were attained for the rechargeable Zn electrode.

Moreover, Lee et al. [231] prepared a mechanically robust CEM for a Zn/Zn symmetric cell by cross-linking polyacrylonitrile (PAN) with lithium polysulfide (equivalent Li_2S_3), simultaneously leading to the formation of sulfur-containing functional fixed groups. This was then followed by hydrolysis, which resulted in the formation of a PAN-S membrane that achieved selective cationic transport (due to the sulfonic functional groups) and a homogeneous ionic flux distribution. As a result, the PAN-S membrane, with a high Young's modulus of 391 MPa, was found to suppress dendrite growth, exhibit a small polarization (<40 mV) and a long cyclic stability (>350 cycles) when tested in the Zn/Zn battery cell.

Another promising method to minimize/avoid the growth of dendrite is to fill the pores of the membranes with chemical compounds that can react with the Zn dendrites and dissolve them. Recently, Xie et al. [232] utilized a 900-μm thick elastomer porous polyolefin membrane (0.1 μm pore size, 58% ± 7.5% porosity) in a Zn-iodine flow battery aiming at overcoming the negative impacts of Zn dendrites. Different compositions of KI, $ZnBr_2$, and KCl were used as electrolytes, thus I^-/I_2 and Zn^{2+}/Zn are the positive and negative redox couples, respectively. The reaction rate of the I_3^-/I^- redox couple was found to be diffusion-limited. The pores of the membranes are believed to be filled with the solution of oxidized I_3^- ions. In this way, the oxidized I_3^- ions are able to oxidize the growing Zn dendrites when entered into the pores and make them soluble again ($Zn + I_3^- \leftrightarrow 3I + Zn^{2+}$). The problem with this system is that I_3^- can diffuse through the membrane and leading to a self-discharge and decrease in coulombic efficiency. Therefore, it is essential to develop and employ a membrane with a proper pore size and/or covered by a thin Nafion® layer faced to the battery positive side [236]. Similar membrane pores functionalization/filling techniques can be considered in Zn-air batteries in order to overcome the adverse effects of Zn-dendrites formation.

5. Summary and outlook

Because of the growing demands for grid-scale electrical energy storage and the inherent attractive attributes of rechargeable Zn-air batteries, such as high theoretical specific energy, high safety, economic feasibility and environmental friendliness, they are considered feasible devices for large-scale electricity storage. The high number of scientific papers published and projects funded so far focused on Zn-air batteries indicates their promising future as next-generation energy storage devices. Membranes have been known to be a critical component of Zn-air batteries as they must selectively transport OH^- ions. Additionally, properly designed membranes should restrict/minimize Zn dendrites formation and growth. This can be achieved by preparing dedicated membranes with an optimal morphology to regulate the ions transport and appropriate chemical modifications to interact and solubilize the dendrites. However, it must be noted that the role of membrane in suppressing Zn-dendrite formations in Zn-air batteries has not been extensively investigated and explored. Therefore, more works on membrane design and investigation of its impact on suppression of dendrite formation and growth are required.

In this review, we have presented and discussed the recent developments in membranes used in Zn-air batteries. The commonly used porous membranes have not been primarily designed for this application, instead, they are adapted from other battery applications. Despite their acceptable OH^- conductivities and chemical stabilities, the crossover of $Zn(OH)_4^{2-}$ ions restricts their widespread usage. Therefore, further research efforts from both researchers and industries on design, fabrication and characterization of high-performance membranes for Zn-air battery are of utmost importance in order to fully commercialize the battery.

One of the strategies used to minimize the crossover of $Zn(OH)_4^{2-}$ ions is the use of properly designed porous membranes specific for Zn-air battery. A porous membrane with an average pore size larger than the hydrated ionic radius of OH^- ions but smaller than that of the $Zn(OH)_4^{2-}$ is needed. Recently, the use of electrospun nanofiber-based porous membranes for rechargeable Zn-air batteries has been introduced in order to improve the membrane integrity. The nanofibers materials fabricated using electrospinning technology have a large surface area, large porosity and favorable molecular orientation along the fiber axis. A promising performance has been reported in the literature.

Another way to inhibit $Zn(OH)_4^{2-}$ ions crossover is by surface modification of porous membranes. The membrane pore size can be decreased by filling the pores with inorganic particles. Membrane coating with inorganic particles has been shown to minimize the Zn $(OH)_4^{2-}$ ions crossover; however, deposition of inorganic particles was reported to also increase the resistance of the membranes. As a result, such membranes have not been commercialized at industrial scale. Hence, an optimum content of inorganic particles not significantly reducing the conductivity of the membrane is required. Coating/filling of porous membranes with ion selective polymers, such as PILs is another promising way to improve their selectivity. This has been reported to block $Zn(OH)_4^{2-}$ crossover from the Zn to the air electrode. However, the high cost of PILs might limit their practical applications. At the same time, this is not well-investigated topic. Hence, more research is needed to explore its potential for practical implementation.

Last but not least, arguably, the most promising approach to reduce $Zn(OH)_4^{2-}$ ions crossover seems to be using ion-selective membranes. Such membranes are able to permeate the OH^- ions while blocking the passage of the larger size $Zn(OH)_4^{2-}$ ions. For instance, the alkaline stable Nafion®, a typical CEM, has been used in Zn-air battery. However, it was reported to exhibit poor performance due to the low OH^- ion conductivity of the membrane. Moreover, it is a well-known that Nafion® is a high cost membrane. Therefore, a CEM with an acceptable conductivity and cost should be considered as an alternative. On the other hand, Nafion® films can be incorporated/coated onto porous membranes to further improve the selectivity of these membranes.

AEMs have been widely proposed to replace the porous membranes used in Zn-air battery applications. It must be noted that since both OH^- and hydrated zincate ions have the same charge, controlling the membrane nanochannels size in a way allowing only OH^- transport is required. The main challenge associated with the use of these membranes is their relatively low alkaline stability. However, this problem is less severe compared to the application of AEMs in high-temperature and low relative humidity fuel cells. Considering the impressive progress nowadays, a promising potential can be foreseen towards the development of low-cost and stable AEMs for the Zn-air battery.

One of the main reasons why Zn-air batteries are considered to be promising energy storage is due to their high specific energy density at a relatively low cost. The material costs of such batteries can be relatively low because Zn is one of the most widely abundant elements and O_2 is merely obtained from air. However, to realize a feasible rechargeable Zn-air battery, reduced cost of the membrane as well as the remaining components of the battery are quite important. The final cost of the membrane highly depends on the raw materials and preparation process.

Funding

This project has received funding from the European Union's Horizon 2020 research and innovation programme under the Marie Skłodowska-Curie Grant Agreement no. 765289.

Declaration of competing interest

The authors declare that they have no known competing financial interests or personal relationships that could have appeared to influence the work reported in this paper.

References

[1] H. Prifti, A. Parasuraman, S. Winardi, T.M. Lim, M. Skyllas-Kazacos, H. Prifti, A. Parasuraman, S. Winardi, T.M. Lim, M. Skyllas-Kazacos, Membranes for redox flow battery applications, Membranes (Basel) 2 (2012) 275–306, https://doi.org/10.3390/membranes2020275.

[2] B. Dunn, H. Kamath, J.-M. Tarascon, Electrical energy storage for the grid: a battery of choices, Science 334 (2011) 928–935, https://doi.org/10.1126/science.1212741.

[3] G.L. Soloveichik, Flow batteries: current status and trends, Chem. Rev. 115 (2015) 11533–11558, https://doi.org/10.1021/cr500720t.

[4] A. Blakers, M. Stocks, B. Lu, C. Cheng, R. Stocks, Pathway to 100% renewable electricity, IEEE J, Photovoltaics 9 (2019) 1828–1833, https://doi.org/10.1109/JPHOTOV.2019.2938882.

[5] W. Wang, Q. Luo, B. Li, X. Wei, L. Li, Z. Yang, Recent progress in redox flow battery research and development, Adv. Funct. Mater. 23 (2013) 970–986, https://doi.org/10.1002/adfm.201200694.

[6] M. Aneke, M. Wang, Energy storage technologies and real life applications – a state of the art review, Appl. Energy 179 (2016) 350–377, https://doi.org/10.1016/J.APENERGY.2016.06.097.

[7] C.W. Chan, J. Ling-Chin, A.P. Roskilly, A review of chemical heat pumps, thermodynamic cycles and thermal energy storage technologies for low grade heat utilisation, Appl. Therm. Eng. 53 (2013) 160–176, https://doi.org/10.1016/J.APPLTHERMALENG.2013.02.030.

[8] P. Pardo, A. Deydier, Z. Anxionnaz-Minvielle, S. Rougé, M. Cabassud, P. Cognet, A review on high temperature thermochemical heat energy storage, Renew. Sustain. Energy Rev. 32 (2014) 591–610, https://doi.org/10.1016/J.RSER.2013.12.014.

[9] J.-M.M. Tarascon, M. Armand, Issues and challenges facing rechargeable lithium batteries, Nature Publishing Group (2001), https://doi.org/10.1038/35104644.

[10] S. Leuthner, Lithium-ion battery overview, in: Lithium-Ion Batter. Basics Appl, Springer, Berlin Heidelberg, 2018, pp. 13–19, https://doi.org/10.1007/978-3-662-53071-9_2.

[11] L. Lu, X. Han, J. Li, J. Hua, M. Ouyang, A review on the key issues for lithium-ion battery management in electric vehicles, J. Power Sources 226 (2013) 272–288, https://doi.org/10.1016/j.jpowsour.2012.10.060.

[12] B. Scrosati, J. Hassoun, Y.K. Sun, Lithium-ion batteries. A look into the future, Energy Environ. Sci. 4 (2011) 3287–3295, https://doi.org/10.1039/c1ee01388b.

[13] G.J. May, A. Davidson, B. Monahov, Lead batteries for utility energy storage: a review, J. Energy Storage 15 (2018) 145–157, https://doi.org/10.1016/j.est.2017.11.008.

[14] L. Gaines, J. Sullivan, A. Burnham, I. Belharouak, Life-cycle analysis of production and recycling of lithium ion batteries, Transport. Res. Rec. (2011) 57–65, https://doi.org/10.3141/2252-08.

[15] RamasamyKulandaivel Saminathan, Lead Acid Battery. Attacking Sulphate Passivation and Cyclability Problems, 2006. http://www.grin.com/en/e-book/373853/lead-acid-battery-attacking-sulphate-pas-. (Accessed 4 May 2020).

[16] R. Ahuja, A. Blomqvist, P. Larsson, P. Pyykkö, P. Zaleski-Ejgierd, Relativity and the lead-acid battery, Phys. Rev. Lett. 106 (2011) 18301, https://doi.org/10.1103/PhysRevLett.106.018301.

[17] P. Ruetschi, Aging mechanisms and service life of lead-acid batteries, in: J. Power Sources, Elsevier, 2004, pp. 33–44, https://doi.org/10.1016/j.jpowsour.2003.09.052.

[18] D. Pavlov, Lead-acid batteries: science and technology a handbook of lead-acid battery technology and its influence on the product, Elsevier (2017), https://doi.org/10.1016/C2012-0-00146-9.

[19] D.A.J. Rand, P.T. Moseley, Energy storage with lead-acid batteries, in: Electrochem. Energy Storage Renew. Sources Grid Balanc, Elsevier Inc., 2015, pp. 201–222, https://doi.org/10.1016/B978-0-444-62616-5.00013-9.

[20] G. May, Secondary batteries –Lead-acid systems: stationary batteries, Encycl. Electrochem. Power Sources 5 (2009) 693–704.

[21] S. Trocino, M. Lo Faro, S.C. Zignani, V. Antonucci, A.S. Aricò, High performance solid-state iron-air rechargeable ceramic battery operating at intermediate temperatures (500–650 °C), Appl. Energy 233–234 (2019) 386–394, https://doi.org/10.1016/j.apenergy.2018.10.022.

[22] D. Gelman, B. Shvartsev, Y. Ein-Eli, Aluminum-air battery based on an ionic liquid electrolyte, J. Mater. Chem. A 2 (2014) 20237–20242, https://doi.org/10.1039/c4ta04721d.

[23] R. Cao, J.-S. Lee, M. Liu, J. Cho, Recent progress in non-precious catalysts for metal-air batteries, Adv. Energy Mater 2 (2012) 816–829, https://doi.org/10.1002/aenm.201200013.

[24] K.F. Blurton, A.F. Sammells, Metal/air batteries: their status and potential - a review, J. Power Sources 4 (1979) 263–279, https://doi.org/10.1016/0378-7753(79)80001-4.

[25] Z.L. Wang, D. Xu, J.J. Xu, X.B. Zhang, Oxygen electrocatalysts in metal-air batteries: from aqueous to nonaqueous electrolytes, Chem. Soc. Rev. 43 (2014) 7746–7786, https://doi.org/10.1039/c3cs60248f.

[26] A.Z. Weber, M.M. Mench, J.P. Meyers, P.N. Ross, J.T. Gostick, Q. Liu, Redox flow batteries: a review, J. Appl. Electrochem. 41 (2011) 1137–1164, https://doi.org/10.1007/s10800-011-0348-2.

[27] B. Hu, C. DeBruler, Z. Rhodes, T.L. Liu, Long-cycling aqueous organic redox flow battery (AORFB) toward sustainable and safe energy storage, J. Am. Chem. Soc. 139 (2017) 1207–1214, https://doi.org/10.1021/jacs.6b10984.

[28] A. Parasuraman, T.M. Lim, C. Menictas, M. Skyllas-Kazacos, Review of material research and development for vanadium redox flow battery applications, Electrochim. Acta 101 (2013) 27–40, https://doi.org/10.1016/j.electacta.2012.09.067.

[29] X. Li, H. Zhang, Z. Mai, H. Zhang, I. Vankelecom, Ion exchange membranes for vanadium redox flow battery (VRB) applications, Energy Environ. Sci. 4 (2011) 1147–1160, https://doi.org/10.1039/c0ee00770f.

[30] K. Lin, R. Gómez-Bombarelli, E.S. Beh, L. Tong, Q. Chen, A. Valle, A. Aspuru-Guzik, M.J. Aziz, R.G. Gordon, A redox-flow battery with an alloxazine-based organic electrolyte, Nat, Energy 1 (2016) 1–8, https://doi.org/10.1038/nenergy.2016.102.

[31] W. Smith, Role of fuel cells in energy storage, J. Power Sources 86 (2000) 74–83, https://doi.org/10.1016/S0378-7753(99)00485-1.

[32] B. Peng, J. Chen, Functional materials with high-efficiency energy storage and conversion for batteries and fuel cells, Coord. Chem. Rev. 253 (2009) 2805–2813, https://doi.org/10.1016/j.ccr.2009.04.008.

[33] J. Bowers, Center for energy efficient materials (CEEM) (final technical report), Argonne, IL (United States) (2014), https://doi.org/10.2172/1169473.

[34] N. Mahmood, C. Zhang, H. Yin, Y. Hou, Graphene-based nanocomposites for energy storage and conversion in lithium batteries, supercapacitors and fuel cells, J. Mater. Chem. A 2 (2014) 15–32, https://doi.org/10.1039/c3ta13033a.

[35] S. Dong, X. Chen, X. Zhang, G. Cui, Nanostructured transition metal nitrides for energy storage and fuel cells, Coord. Chem. Rev. 257 (2013) 1946–1956, https://doi.org/10.1016/j.ccr.2012.12.012.

[36] W. Vielstich, A. Lamm, HubertA. Gasteiger, H. Yokokawa, Handbook of Fuel Cells ;: Fundamentals, Technology, and Applications, Wiley, 2003.

[37] C. Abbey, G. Joos, Supercapacitor energy storage for wind energy applications, IEEE Trans. Ind. Appl. 43 (2007) 769–776, https://doi.org/10.1109/TIA.2007.895768.

[38] L. Qu, W. Qiao, Constant power control of DFIG wind turbines with supercapacitor energy storage, IEEE Trans. Ind. Appl. 47 (2011) 359–367, https://doi.org/10.1109/TIA.2010.2090932.

[39] W. Li, G. Joós, J. Bélanger, Real-time simulation of a wind turbine generator coupled with a battery supercapacitor energy storage system, IEEE Trans. Ind. Electron. 57 (2010) 1137–1145, https://doi.org/10.1109/TIE.2009.2037103.

[40] B.E. Conway, Transition from "supercapacitor" to "battery" behavior in electrochemical energy storage, J. Electrochem. Soc. 138 (1991) 1539, https://doi.org/10.1149/1.2085829.

[41] T. Ma, H. Yang, L. Lu, Development of hybrid battery-supercapacitor energy storage for remote area renewable energy systems, Appl. Energy 153 (2015) 56–62, https://doi.org/10.1016/j.apenergy.2014.12.008.

[42] D.P. Dubal, O. Ayyad, V. Ruiz, P. Gómez-Romero, Hybrid energy storage: the merging of battery and supercapacitor chemistries, Chem. Soc. Rev. 44 (2015) 1777–1790, https://doi.org/10.1039/c4cs00266k.

[43] J. Yi, P. Liang, X. Liu, K. Wu, Y. Liu, Y. Wang, Y. Xia, J. Zhang, Challenges, mitigation strategies and perspectives in development of zinc-electrode materials and fabrication for rechargeable zinc–air batteries, Energy Environ. Sci. 11 (2018) 3075–3095, https://doi.org/10.1039/C8EE01991F.

[44] Y. Li, H. Dai, Recent advances in zinc–air batteries, Chem. Soc. Rev. 43 (2014) 5257–5275, https://doi.org/10.1039/C4CS00015C.

[45] P. Tan, B. Chen, H. Xu, H. Zhang, W. Cai, M. Ni, M. Liu, Z. Shao, Flexible Zn– and Li–air batteries: recent advances, challenges, and future perspectives, Energy Environ. Sci. 10 (2017) 2056–2080, https://doi.org/10.1039/C7EE01913K.

[46] M.A. Rahman, X. Wang, C. Wen, High energy density metal-air batteries: a review, J. Electrochem. Soc. 160 (2013) A1759–A1771, https://doi.org/10.1149/2.062310jes.

[47] A.R. Mainar, O. Leonet, M. Bengoechea, I. Boyano, I. de Meatza, A. Kvasha, A. Guerfi, J. Alberto Blázquez, Alkaline aqueous electrolytes for secondary zinc-air batteries: an overview, Int. J. Energy Res. 40 (2016) 1032–1049, https://doi.org/10.1002/er.3499.

[48] P. Sapkota, H. Kim, Zinc–air fuel cell, a potential candidate for alternative energy, J. Ind. Eng. Chem. 15 (2009) 445–450, https://doi.org/10.1016/J.JIEC.2009.01.002.

[49] J.J. Xu, H. Ye, J. Huang, Novel zinc ion conducting polymer gel electrolytes based on ionic liquids, Electrochem. Commun. 7 (2005) 1309–1317, https://doi.org/10.1016/J.ELECOM.2005.09.011.

[50] P. Pei, K. Wang, Z. Ma, Technologies for extending zinc–air battery's cyclelife: a review, Appl. Energy 128 (2014) 315–324, https://doi.org/10.1016/J.APENERGY.2014.04.095.

[51] J.-S. Lee, S. Tai Kim, R. Cao, N.-S. Choi, M. Liu, K.T. Lee, J. Cho, Metal-air batteries with high energy density: Li-air versus Zn-air, Adv. Energy Mater 1 (2011) 34–50, https://doi.org/10.1002/aenm.201000010.

[52] D. Linden, T.B. Reddy, Handbook of Batteries, McGraw-Hill, 2002.

[53] D. Stock, S. Dongmo, J. Janek, D. Schröder, Benchmarking anode concepts: the future of electrically rechargeable zinc-air batteries, ACS Energy Lett. 4 (2019) 1287–1300, https://doi.org/10.1021/acsenergylett.9b00510.

[54] J.F. Drillet, F. Holzer, T. Kallis, S. Müller, V.M. Schmidt, Influence of CO2 on the stability of bifunctional oxygen electrodes for rechargeable zinc/air batteries and study of different CO2 filter materials, in: Phys. Chem. Chem. Phys, Royal Society of Chemistry, 2001, pp. 368–371, https://doi.org/10.1039/b005523i.

[55] M.A. Al-Saleh, S. Gültekin, A.S. Al-Zakri, H. Celiker, Effect of carbon dioxide on the performance of Ni/PTFE and Ag/PTFE electrodes in an alkaline fuel cell, J. Appl. Electrochem. 24 (1994) 575–580, https://doi.org/10.1007/BF00249861.

[56] H.H. Cheng, C.S. Tan, Reduction of CO2 concentration in a zinc/air battery by absorption in a rotating packed bed, J. Power Sources 162 (2006) 1431–1436, https://doi.org/10.1016/j.jpowsour.2006.07.046.

[57] E. Gülzow, Alkaline fuel cells: a critical view, J. Power Sources 61 (1996) 99–104, https://doi.org/10.1016/S0378-7753(96)02344-0.

[58] E.B. Fox, H.R. Colón-Mercado, Y. Chen, W.S.W. Ho, Development and selection of ionic liquid electrolytes for hydroxide conducting polybenzimidazole membranes in alkaline fuel cells, in: ACS Symp. Ser, American Chemical Society, 2012, pp. 129–143, https://doi.org/10.1021/bk-2012-1117.ch005.

[59] U. Krewer, C. Weinzierl, N. Ziv, D.R. Dekel, Impact of carbonation processes in anion exchange membrane fuel cells, Electrochim. Acta 263 (2018) 433–446, https://doi.org/10.1016/j.electacta.2017.12.093.

[60] Technology and IP, Wattech Power, n.d, http://www.wattechpower.com/technology. (Accessed 15 March 2019).

[61] F.R. McLarnon, E.J. Cairns, Zinc–air Battery: understanding the structure and morphology changes of graphene-supported CoMn2O4 bifunctional catalysts under practical rechargeable conditions, J. Electrochem. Soc. 138 (1991) 645, https://doi.org/10.1149/1.2085653.

[62] A.M. Bernardes, D.C.R. Espinosa, J.A.S. Tenório, Recycling of batteries: a review of current processes and technologies, J. Power Sources 130 (2004) 291–298, https://doi.org/10.1016/j.jpowsour.2003.12.026.

[63] J. Fu, Z.P. Cano, M.G. Park, A. Yu, M. Fowler, Z. Chen, Electrically rechargeable zinc–air batteries: progress, challenges, and perspectives, Adv. Mater. 29 (2017), https://doi.org/10.1002/adma.201604685.

[64] V. Caramia, B. Bozzini, Materials science aspects of zinc–air batteries: a review, Mater. Renew. Sustain. Energy 3 (2014) 28, https://doi.org/10.1007/s40243-014-0028-3.

[65] J. Pan, Y.Y. Xu, H. Yang, Z. Dong, H. Liu, B.Y. Xia, Advanced architectures and relatives of air electrodes in Zn-air batteries, Adv. Sci. 5 (2018) 1700691, https://doi.org/10.1002/advs.201700691.

[66] Q. Liu, Z. Pan, E. Wang, L. An, G. Sun, Aqueous metal-air batteries: fundamentals and applications, Energy Storage Mater (2019), https://doi.org/10.1016/j.ensm.2019.12.011.

[67] E. Davari, D.G. Ivey, Bifunctional electrocatalysts for Zn-air batteries, Sustain. Energy Fuels 2 (2018) 39–67, https://doi.org/10.1039/c7se00413c.

[68] J. Zhang, Q. Zhou, Y. Tang, L. Zhang, Y. Li, Zinc-air batteries: are they ready for prime time? Chem. Sci. 10 (2019) 8924–8929, https://doi.org/10.1039/c9sc04221k.

[69] G. Toussaint, P. Stevens, L. Akrour, R. Rouget, F. Fourgeot, Development of a rechargeable zinc-air battery, in: ECS Trans, ECS, 2010, pp. 25–34, https://doi.org/10.1149/1.3507924.

[70] Y. Li, M. Gong, Y. Liang, J. Feng, J.E. Kim, H. Wang, G. Hong, B. Zhang, H. Dai, Advanced zinc-air batteries based on high-performance hybrid electrocatalysts, Nat. Commun. 4 (2013) 1–7, https://doi.org/10.1038/ncomms2812.

[71] A.R. Mainar, E. Iruin, L.C. Colmenares, A. Kvasha, I. de Meatza, M. Bengoechea, O. Leonet, I. Boyano, Z. Zhang, J.A. Blazquez, An overview of progress in electrolytes for secondary zinc-air batteries and other storage systems based on zinc, J. Energy Storage 15 (2018) 304–328, https://doi.org/10.1016/j.est.2017.12.004.

[72] M. Hilder, B. Winther-Jensen, N.B. Clark, The effect of binder and electrolyte on the performance of thin zinc-air battery, Electrochim. Acta 69 (2012) 308–314, https://doi.org/10.1016/j.electacta.2012.03.004.

[73] Z. Chen, J.-Y. Choi, H. Wang, H. Li, Z. Chen, Highly durable and active non-precious air cathode catalyst for zinc air battery, J. Power Sources 196 (2011) 3673–3677, https://doi.org/10.1016/j.jpowsour.2010.12.047.

[74] S. Zhu, Z. Chen, B. Li, D. Higgins, H. Wang, H. Li, Z. Chen, Nitrogen-doped carbon nanotubes as air cathode catalysts in zinc-air battery, Electrochim. Acta 56 (2011) 5080–5084, https://doi.org/10.1016/j.electacta.2011.03.082.

[75] V. Neburchilov, H. Wang, J.J. Martin, W. Qu, A review on air cathodes for zinc–air fuel cells, J. Power Sources 195 (2010) 1271–1291, https://doi.org/10.1016/j.jpowsour.2009.08.100.

[76] X.G. Zhang, Fibrous zinc anodes for high power batteries, J. Power Sources 163 (2006) 591–597, https://doi.org/10.1016/j.jpowsour.2006.09.034.

[77] C.W. Lee, K. Sathiyanarayanan, S.W. Eom, M.S. Yun, Novel alloys to improve the electrochemical behavior of zinc anodes for zinc/air battery, J. Power Sources 160 (2006) 1436–1441, https://doi.org/10.1016/j.jpowsour.2006.02.019.

[78] X.-B. Zhang, Metal-air Batteries : Fundamentals and Applications, 2018.

[79] P. Sapkota, H. Kim, An experimental study on the performance of a zinc air fuel cell with inexpensive metal oxide catalysts and porous organic polymer separators, J. Ind. Eng. Chem. 16 (2010) 39–44, https://doi.org/10.1016/j.jiec.2010.01.024.

[80] W. Lu, C. Xie, H. Zhang, X. Li, Inhibition of zinc dendrite growth in zinc-based batteries, ChemSusChem. 11 (2018) 3996–4006, https://doi.org/10.1002/cssc.201801657.

[81] C. Chakkaravarthy, A.K.A. Waheed, H.V.K. Udupa, Zinc-air alkaline batteries - a review, J. Power Sources 6 (1981) 203–228, https://doi.org/10.1016/0378-7753(81)80027-4.

[82] Y. Zhang, C. Li, X. Cai, J. Yao, M. Li, X. Zhang, Q. Liu, High alkaline tolerant electrolyte membrane with improved conductivity and mechanical strength via lithium chloride/dimethylacetamide dissolved microcrystalline cellulose for Zn-Air batteries, Electrochim. Acta 220 (2016) 635–642, https://doi.org/10.1016/j.electacta.2016.10.103.

[83] H.J. Hwang, W.S. Chi, O. Kwon, J.G. Lee, J.H. Kim, Y.G. Shul, Selective ion transporting polymerized ionic liquid membrane separator for enhancing cycle stability and durability in secondary zinc-air battery systems, ACS Appl. Mater. Interfaces 8 (2016) 26298–26308, https://doi.org/10.1021/acsami.6b07841.

[84] E.L. Dewi, K. Oyaizu, H. Nishide, E. Tsuchida, Cationic polysulfonium membrane as separator in zinc-air cell, J. Power Sources 115 (2003) 149–152, https://doi.org/10.1016/S0378-7753(02)00650-X.

[85] H.J. Lee, J.M. Lim, H.W. Kim, S.H. Jeong, S.W. Eom, Y.T. Hong, S.Y. Lee, Electrospun polyetherimide nanofiber mat-reinforced, permselective polyvinyl alcohol composite separator membranes: a membrane-driven step closer toward rechargeable zinc-air batteries, J. Membr. Sci. 499 (2016) 526–537, https://doi.org/10.1016/j.memsci.2015.10.038.

[86] H.W. Kim, J.M. Lim, H.J. Lee, S.W. Eom, Y.T. Hong, S.Y. Lee, Artificially engineered, bicontinuous anion-conducting/-repelling polymeric phases as a selective ion transport channel for rechargeable zinc-air battery separator membranes, J. Mater. Chem. A 4 (2016) 3711–3720, https://doi.org/10.1039/c5ta09576j.

[87] W.J. Koros, Gas separation membranes: needs for combined materials science and processing approaches, Macromol. Symp. 188 (2002) 13–22, https://doi.org/10.1002/1521-3900(200211)188:1<13::AID-MASY13>3.0.CO;2-W.

[88] L. Gubler, Membranes and separators for redox flow batteries, Curr. Opin. Electrochem 18 (2019) 31–36, https://doi.org/10.1016/j.coelec.2019.08.007.

[89] Geert-H. Koops, Nomenclature and Symbols in Membrane Science and Technology : on Behalf of the European Society of Membrane Science and Technology, Membrane Technology Group, University of Twente, 1995.

[90] M. Mulder, M. Mulder, Introduction, in: Basic Princ, Membr. Technol., Springer Netherlands, 1996, pp. 1–21, https://doi.org/10.1007/978-94-009-1766-8_1.

[91] B. Van Der Bruggen, C. Vandecasteele, T. Van Gestel, W. Doyen, R. Leysen, A review of pressure-driven membrane processes in wastewater treatment and drinking water production, Environ. Prog. 22 (2003) 46–56, https://doi.org/10.1002/ep.670220116.

[92] P. Arribas, M. Khayet, M.C. García-Payo, L. Gil, Advances in Membrane Technologies for Water Treatment (Chapter 8) Novel and Emerging Membranes, Elsevier, 2015, https://doi.org/10.1016/B978-1-78242-121-4.00008-3.

[93] A. Zirehpour, A. Rahimpour, Nanostructured polymer membranes, in: V.P.M. O. Nazarenko (Ed.), Nanostructured Polym. Membr, vol. 2, Appl., Scrivener, 2016, p. 560.

[94] H. Strathmann, L. Giorno, E. Drioli, An Introduction to Membrane Science and Technology, 2006.

[95] M. Ulbricht, Nanoporous polymer filters and membranes, selective filters, in: Encycl. Polym. Nanomater, Springer Berlin Heidelberg, Berlin, Heidelberg, 2015, pp. 1360–1371, https://doi.org/10.1007/978-3-642-29648-2_357.

[96] K.S.W. Sing, D.H. Everett, R.A.W. Haul, L. Moscou, R.A. Pierotti, J. Rouquerol, T. Siemieniewska, Reporting physisorption data for gas/solid systems with special reference to the determination of surface area and porosity, Pure Appl. Chem. 57 (1985) 603–619, https://doi.org/10.1351/pac198557040603.

[97] D.M. See, R.E. White, Temperature and concentration dependence of the specific conductivity of concentrated solutions of potassium hydroxide, J. Chem. Eng. Data 42 (1997) 1266–1268, https://doi.org/10.1021/je970140x.

[98] R.J. Gilliam, J.W. Graydon, D.W. Kirk, S.J. Thorpe, A review of specific conductivities of potassium hydroxide solutions for various concentrations and temperatures, Int. J. Hydrogen Energy 32 (2007) 359–364, https://doi.org/10.1016/j.ijhydene.2006.10.062.

[99] X.G. Zhang, Corrosion and electrochemistry of zinc, in: Corros. Electrochem. Zinc, Springer US, Boston, MA, 1996, pp. 1–17, https://doi.org/10.1007/978-1-4757-9877-7_1.

[100] S. Hosseini, S.J. Han, A. Arponwichanop, T. Yonezawa, S. Kheawhom, Ethanol as an electrolyte additive for alkaline zinc-air flow batteries, Sci. Rep. 8 (2018) 1–11, https://doi.org/10.1038/s41598-018-29630-0.

[101] M. Xu, D.G. Ivey, Z. Xie, W. Qu, Rechargeable Zn-air batteries: progress in electrolyte development and cell configuration advancement, J. Power Sources 283 (2015) 358–371, https://doi.org/10.1016/j.jpowsour.2015.02.114.

[102] D.R. Dekel, Review of cell performance in anion exchange membrane fuel cells, J. Power Sources 375 (2018) 158–169, https://doi.org/10.1016/j.jpowsour.2017.07.117.

[103] S. Maurya, S.H. Shin, Y. Kim, S.H. Moon, A review on recent developments of anion exchange membranes for fuel cells and redox flow batteries, RSC Adv. 5 (2015) 37206–37230, https://doi.org/10.1039/c5ra04741b.

[104] S. Gottesfeld, D.R. Dekel, M. Page, C. Bae, Y. Yan, P. Zelenay, Y.S. Kim, Anion exchange membrane fuel cells: current status and remaining challenges, J. Power Sources 375 (2018) 170–184, https://doi.org/10.1016/j.jpowsour.2017.08.010.

[105] G. Merle, M. Wessling, K. Nijmeijer, Anion exchange membranes for alkaline fuel cells: a review, J. Membr. Sci. 377 (2011) 1–35, https://doi.org/10.1016/J.MEMSCI.2011.04.043.

[106] W. You, K.J.T. Noonan, G.W. Coates, Alkaline-stable anion exchange membranes: a review of synthetic approaches, Prog, Polym. Sci. 100 (2020) 101177, https://doi.org/10.1016/j.progpolymsci.2019.101177.
[107] Y.J. Wang, J. Qiao, R. Baker, J. Zhang, Alkaline polymer electrolyte membranes for fuel cell applications, Chem. Soc. Rev. 42 (2013) 5768–5787, https://doi.org/10.1039/c3cs60053j.
[108] S.C. Ramírez, R.R. Paz, Hydroxide transport in anion-exchange membranes for alkaline fuel cells, in: New Trends Ion Exch. Stud, InTech, 2018, https://doi.org/10.5772/intechopen.77148.
[109] D. Dong, W. Zhang, A.C.T. Van Duin, D. Bedrov, Grotthuss versus vehicular transport of hydroxide in anion-exchange membranes: insight from combined reactive and nonreactive molecular simulations, J. Phys. Chem. Lett. 9 (2018) 825–829, https://doi.org/10.1021/acs.jpclett.8b00004.
[110] K.N. Grew, W.K.S. Chiu, A dusty fluid model for predicting hydroxyl anion conductivity in alkaline anion exchange membranes, J. Electrochem. Soc. 157 (2010), https://doi.org/10.1149/1.3273200. B327.
[111] M.E. Tuckerman, A. Chandra, D. Marx, Structure and dynamics of OH - (aq), Acc. Chem. Res. 39 (2006) 151–158, https://doi.org/10.1021/ar040207n.
[112] M.E. Tuckerman, D. Marx, M. Parrinello, The nature and transport mechanism of hydrated hydroxide ions in aqueous solution, Nature 417 (2002) 925–929, https://doi.org/10.1038/nature00797.
[113] H. Takaba, T. Hisabe, T. Shimizu, M.K. Alam, Molecular modeling of OH− transport in poly(arylene ether sulfone ketone)s containing quaternized ammonio-substituted fluorenyl groups as anion exchange membranes, J. Membr. Sci. 522 (2017) 237–244, https://doi.org/10.1016/j.memsci.2016.09.019.
[114] D. Marx, A. Chandra, M.E. Tuckerman, Aqueous basic solutions: hydroxide solvation, structural diffusion, and comparison to the hydrated proton, Chem. Rev. 110 (2010) 2174–2216, https://doi.org/10.1021/cr900233f.
[115] Grotthuss mechanism, n.d, http://www1.lsbu.ac.uk/water/grotthuss.html. (Accessed 22 June 2020).
[116] D.S. Kim, G.P. Robertson, Y.S. Kim, M.D. Guiver, Copoly(arylene ether)s containing pendant sulfonic acid groups as proton exchange membranes, Macromolecules 42 (2009) 957–963, https://doi.org/10.1021/ma802192y.
[117] F. Song, Y. Fu, Y. Gao, J. Li, J. Qiao, X.D. Zhou, Y. Liu, Novel alkaline anion-exchange membranes based on chitosan/ethenylmethylimidazoliumchloride polymer with ethenylpyrrolidone composites for low temperature polymer electrolyte fuel cells, Electrochim. Acta 177 (2015) 137–144, https://doi.org/10.1016/j.electacta.2015.02.015.
[118] P. Choi, N.H. Jalani, R. Datta, Thermodynamics and proton transport in nafion, J. Electrochem. Soc. 152 (2005), https://doi.org/10.1149/1.1859814. E123.
[119] X. Fan, J. Liu, J. Ding, Y. Deng, X. Han, W. Hu, C. Zhong, Investigation of the environmental stability of poly(vinyl alcohol)–KOH polymer electrolytes for flexible zinc–air batteries, Front. Chem 7 (2019), https://doi.org/10.3389/fchem.2019.00678.
[120] R. Naderi, Composite gel polymer electrolyte for lithium ion batteries. http://openprairie.sdstate.edu/etd, 2016. (Accessed 22 June 2020).
[121] M. Wang, N. Xu, J. Fu, Y. Liu, J. Qiao, High-performance binary cross-linked alkaline anion polymer electrolyte membranes for all-solid-state supercapacitors and flexible rechargeable zinc-air batteries, J. Mater. Chem. A 7 (2019) 11257–11264, https://doi.org/10.1039/c9ta02314c.
[122] J. Zhang, T. Zhou, J. Qiao, Y. Liu, J. Zhang, Hydroxyl anion conducting membranes poly(vinyl alcohol)/poly(diallyldimethylammonium chloride) for alkaline fuel cell applications: effect of molecular weight, Electrochim. Acta 111 (2013) 351–358, https://doi.org/10.1016/j.electacta.2013.07.182.
[123] J.O. Bockris, Z. Nagy, A. Damjanovic, On the deposition and dissolution of zinc in alkaline solutions, J. Electrochem. Soc. 119 (1972) 285, https://doi.org/10.1149/1.2404188.
[124] W.G. Sunu, D.N. Bennion, Transient and failure analyses of the porous zinc electrode, J. Electrochem. Soc. 127 (1980) 2017, https://doi.org/10.1149/1.2130055.
[125] P. Gu, M. Zheng, Q. Zhao, X. Xiao, H. Xue, H. Pang, Rechargeable zinc-air batteries: a promising way to green energy, J. Mater. Chem. A 5 (2017) 7651–7666, https://doi.org/10.1039/c7ta01693j.
[126] E. Jorge Pessine, S.M.L. Agostinho, L.I.O.C. Chagas, Evaluation of the diffusion coefficient of the zincate ion using a rotating disk electrode, n.d, www.nrcresearchpress.com. (Accessed 4 February 2020).
[127] E.R. Nightingale, Phenomenological theory of ion solvation. Effective radii of hydrated ions, J. Phys. Chem. 63 (1959) 1381–1387, https://doi.org/10.1021/j150579a011.
[128] T. Luo, S. Abdu, M. Wessling, Selectivity of ion exchange membranes: a review. https://www.sciencedirect.com/science/article/pii/S0376738817335779, 2018. (Accessed 28 April 2019).
[129] Y. Li, S. Gregory, Diffusion of ions in sea water and in deep-sea sediments, Geochem. Cosmochim. Acta 38 (1974) 703–714.
[130] W. Haynes, CRC Handbook of Chemistry and Physics, 96th ed., CRC Press, CRC Press, Taylor & Francis Group, Boca Raton, London, New York, 2015.
[131] J. Xi, Z. Wu, X. Teng, Y. Zhao, L. Chen, X. Qiu, Self-assembled polyelectrolyte multilayer modified Nafion membrane with suppressed vanadium ion crossover for vanadium redox flow batteries, J. Mater. Chem. 18 (2008) 1232, https://doi.org/10.1039/b718526j.
[132] H. Zhang, H. Zhang, X. Li, Z. Mai, W. Wei, Silica modified nanofiltration membranes with improved selectivity for redox flow battery application, Energy Environ. Sci. 5 (2012) 6299–6303, https://doi.org/10.1039/C1EE02571F.
[133] H. Zhang, H. Zhang, X. Li, Z. Mai, J. Zhang, Nanofiltration (NF) membranes: the next generation separators for all vanadium redox flow batteries (VRBs)? Energy Environ. Sci. 4 (2011) 1676, https://doi.org/10.1039/c1ee01117k.
[134] J. Duay, M. Kelly, T.N. Lambert, Evaluation of a ceramic separator for use in rechargeable alkaline Zn/MnO2 batteries, J. Power Sources 395 (2018) 430–438, https://doi.org/10.1016/j.jpowsour.2018.05.072.
[135] I. Krejčí, P. Vanýsek, A. Trojánek, Transport of Zn (OH)42- ions across a polyolefin microporous membrane, J. Electrochem. Soc. 140 (1993) 2279, https://doi.org/10.1149/1.2220808.
[136] J. Duay, T.N. Lambert, R. Aidun, Stripping voltammetry for the real time determination of zinc membrane diffusion coefficients in high pH: towards rapid screening of alkaline battery separators, Electroanalysis 29 (2017) 2261–2267, https://doi.org/10.1002/elan.201700337.
[137] H. Lee, M. Yanilmaz, O. Toprakci, K. Fu, X. Zhang, A review of recent developments in membrane separators for rechargeable lithium-ion batteries. http://xlink.rsc.org/?DOI=C4EE01432D, 2014. (Accessed 28 April 2019).
[138] M.R. Palacín, Recent advances in rechargeable battery materials: a chemist's perspective, Chem. Soc. Rev. 38 (2009) 2565, https://doi.org/10.1039/b820555h.
[139] R. Narducci, J.-F. Chailan, A. Fahs, L. Pasquini, M.L. Di Vona, P. Knauth, Mechanical properties of anion exchange membranes by combination of tensile stress-strain tests and dynamic mechanical analysis, J. Polym. Sci. Part B Polym. Phys. 54 (2016) 1180–1187, https://doi.org/10.1002/polb.24025.
[140] P. A, Z.John Zhang, Battery Separators, Chemical Reviews, 2004, https://doi.org/10.1021/CR020738U.
[141] S.S. Zhang, A review on the separators of liquid electrolyte Li-ion batteries, J. Power Sources 164 (2007) 351–364, https://doi.org/10.1016/j.jpowsour.2006.10.065.
[142] J. Fu, J. Zhang, X. Song, H. Zarrin, X. Tian, J. Qiao, L. Rasen, K. Li, Z. Chen, A flexible solid-state electrolyte for wide-scale integration of rechargeable zinc-air batteries, Energy Environ. Sci. 9 (2016) 663–670, https://doi.org/10.1039/c5ee03404c.
[143] J. Zhang, J. Fu, X. Song, G. Jiang, H. Zarrin, P. Xu, K. Li, A. Yu, Z. Chen, Laminated cross-linked nanocellulose/graphene oxide electrolyte for flexible rechargeable zinc-air batteries, Adv. Energy Mater 6 (2016) 1600476, https://doi.org/10.1002/aenm.201600476.
[144] H. Zarrin, S. Sy, J. Fu, G. Jiang, K. Kang, Y.-S. Jun, A. Yu, M. Fowler, Z. Chen, Molecular functionalization of graphene oxide for next-generation wearable electronics, ACS Appl. Mater. Interfaces 8 (2016) 25428–25437, https://doi.org/10.1021/acsami.6b06769.
[145] Y. Wei, M. Wang, N. Xu, L. Peng, J. Mao, Q. Gong, J. Qiao, Alkaline exchange polymer membrane electrolyte for high performance of all-solid-state electrochemical devices, ACS Appl. Mater. Interfaces 10 (2018) 29593–29598, https://doi.org/10.1021/acsami.8b09545.
[146] J. Fang, J. Qiao, D.P. Wilkinson, J. Zhang, Electrochemical Polymer Electrolyte Membranes, CRC Press, 2015.
[147] S. Hosseini, W. Lao-atiman, S.J. Han, A. Arpornwichanop, T. Yonezawa, S. Kheawhom, Discharge performance of zinc-air flow Bbatteries under the effects of sodium dodecyl sulfate and pluronic F-127, Sci. Rep. 8 (2018) 14909, https://doi.org/10.1038/s41598-018-32806-3.
[148] W. Lao-Atiman, S. Olaru, A. Arpornwichanop, S. Kheawhom, Discharge performance and dynamic behavior of refuellable zinc-air battery, Sci. Data 6 (2019) 168, https://doi.org/10.1038/s41597-019-0178-3.
[149] P. Kritzer, J.A. Cook, Nonwovens as separators for alkaline batteries, A481, J. Electrochem. Soc. 154 (2007), https://doi.org/10.1149/1.2711064.
[150] K. Liu, Y. Liu, D. Lin, A. Pei, Y. Cui, Materials for lithium-ion battery safety, Sci. Adv 4 (2018), https://doi.org/10.1126/sciadv.aas9820.
[151] W. Peng, I.C. Escobar, D.B. White, Effects of water chemistries and properties of membrane on the performance and fouling—a model development study, J. Membr. Sci. 238 (2004) 33–46, https://doi.org/10.1016/j.memsci.2004.02.035.
[152] C.C. Yang, G.M. Wu, Study of microporous PVA/PVC composite polymer membrane and it application to MnO2 capacitors, Mater. Chem. Phys. 114 (2009) 948–955, https://doi.org/10.1016/j.matchemphys.2008.11.009.
[153] L.L.C. Celgard, Celgard High Performance Battery Separators, vol. 2200, 2009.
[154] F. Cheng, J. Chen, Metal–air batteries: from oxygen reduction electrochemistry to cathode catalysts, Chem. Soc. Rev. 41 (2012) 2172, https://doi.org/10.1039/c1cs15228a.
[155] A. Abbasi, S. Hosseini, A. Somwangthanaroj, A.A. Mohamad, S. Kheawhom, Poly (2,6-Dimethyl-1,4-Phenylene Oxide)-based hydroxide exchange separator membranes for zinc–air battery, Int. J. Mol. Sci. 20 (2019) 3678, https://doi.org/10.3390/ijms20153678.
[156] Y. Kiros, Separation and permeability of zincate ions through membranes, J. Power Sources 62 (1996) 117–119, https://doi.org/10.1016/S0378-7753(96)02420-2.
[157] D.E. Turney, J.W. Gallaway, G.G. Yadav, R. Ramirez, M. Nyce, S. Banerjee, Y.C. K. Chen-Wiegart, J. Wang, M.J. D'Ambrose, S. Kolhekar, J. Huang, X. Wei, Rechargeable zinc alkaline anodes for long-cycle energy storage, Chem. Mater. 29 (2017) 4819–4832, https://doi.org/10.1021/acs.chemmater.7b00754.
[158] O.C. Wagner, Secondary Zinc-Air Cell Investigations, 1972.
[159] Technical properties (typical values), n.d, www.innoviafilms.com. (Accessed 16 March 2020).
[160] B. Seymour, Cellophane membrane permeability, J. Biol. Chem. (1940) 701–707.
[161] W. Cao, Y. Li, B. Fitch, J. Shih, T. Doung, J. Zheng, Strategies to optimize lithium-ion supercapacitors achieving high-performance: cathode configurations, lithium loadings on anode, and types of separator, J. Power Sources 268 (2014) 841–847, https://doi.org/10.1016/j.jpowsour.2014.06.090.
[162] J. Huang, G.G. Yadav, J. Gallaway, M. Nyce, S. Banerjee, Rechargeable Alkaline Battery Comprising Metal Hydroxide Separator, 2019.

[163] K. Trommer, B. Morgenstern, Nonrigid microporous PVC sheets: preparation and properties, J. Appl. Polym. Sci. 115 (2010) 2119–2126, https://doi.org/10.1002/app.31305.

[164] M. Ulbricht, Advanced functional polymer membranes, Polymer (Guildf) 47 (2006) 2217–2262, https://doi.org/10.1016/j.polymer.2006.01.084.

[165] E. Drioli, L. Giorno, Membrane Operations: Innovative Separations and Transformations, Wiley-VCH, 2009, https://doi.org/10.1002/9783527626779.

[166] M. Mulder, Phase inversion membranes, in: Ian D. Wilson (Ed.), Encycl. Sep. Sci., Academic Press, 2000, 3331–3331.

[167] F. Liu, N.A. Hashim, Y. Liu, M.R.M. Abed, K. Li, Progress in the production and modification of PVDF membranes, J. Membr. Sci. 375 (2011) 1–27, https://doi.org/10.1016/j.memsci.2011.03.014.

[168] C.C. Yang, J.M. Yang, C.Y. Wu, Poly(vinyl alcohol)/poly(vinyl chloride) composite polymer membranes for secondary zinc electrodes, J. Power Sources 191 (2009) 669–677, https://doi.org/10.1016/j.jpowsour.2009.02.044.

[169] G.M. Wu, S.J. Lin, C.C. Yang, Alkaline Zn-air and Al-air cells based on novel solid PVA/PAA polymer electrolyte membranes, J. Membr. Sci. 280 (2006) 802–808, https://doi.org/10.1016/J.MEMSCI.2006.02.037.

[170] A. Puapattanakul, S. Therdthianwong, A. Therdthianwong, N. Wongyao, Improvement of zinc-air fuel cell performance by gelled koh, Energy Procedia 34 (2013) 173–180, https://doi.org/10.1016/j.egypro.2013.06.745.

[171] C.C. Yang, S.J. Lin, S.T. Hsu, Synthesis and characterization of alkaline polyvinyl alcohol and poly(epichlorohydrin) blend polymer electrolytes and performance in electrochemical cells, J. Power Sources 122 (2003) 210–218, https://doi.org/10.1016/S0378-7753(03)00429-4.

[172] J.R. Kim, S.W. Choi, S.M. Jo, W.S. Lee, B.C. Kim, Electrospun PVdF-based fibrous polymer electrolytes for lithium ion polymer batteries, Electrochim. Acta 50 (2004) 69–75, https://doi.org/10.1016/j.electacta.2004.07.014.

[173] S.W. Choi, S.M. Jo, W.S. Lee, Y.-R. Kim, An electrospun poly(vinylidene fluoride) nanofibrous membrane and its battery applications, Adv. Mater. 15 (2003) 2027–2032, https://doi.org/10.1002/adma.200304617.

[174] B. Ding, J. Yu, X. Wang, Electrospinning: Nanofabrication and Applications, Elsevier, 2018, https://doi.org/10.1016/C2016-0-01374-8.

[175] V.G. Gude, Emerging Technologies for Sustainable Desalination Handbook, Elsevier, 2018, https://doi.org/10.1016/C2017-0-03562-0.

[176] T.H. Cho, M. Tanaka, H. Ohnishi, Y. Kondo, M. Yoshikazu, T. Nakamura, T. Sakai, Composite nonwoven separator for lithium-ion battery: development and characterization, J. Power Sources 195 (2010) 4272–4277, https://doi.org/10.1016/j.jpowsour.2010.01.018.

[177] J. Zhang, Z. Liu, Q. Kong, C. Zhang, S. Pang, L. Yue, X. Wang, J. Yao, G. Cui, Renewable and superior thermal-resistant cellulose-based composite nonwoven as lithium-ion battery separator, ACS Appl. Mater. Interfaces 5 (2013) 128–134, https://doi.org/10.1021/am302290n.

[178] G. Zguris, A broad look at separator material technology for valve-regulated lead/acid batteries, J. Power Sources 73 (1998) 60–64, https://doi.org/10.1016/S0378-7753(98)00022-6.

[179] S.J. H, S.K. Ali Abbasia, Soraya Hosseinia, Discharge capacity improvement of zinc-air battery using electrospun polypropylene nanofibrous separator, in: ECS Meet. Abstr, 2019. MA2019-04, http://ma.ecsdl.org/content/MA2019-04/5/229.short. (Accessed 30 January 2020).

[180] J. Noack, N. Roznyatovskaya, T. Herr, P. Fischer, The chemistry of redox-flow batteries, Angew. Chemie Int 54 (2015) 9776–9809, https://doi.org/10.1002/anie.201410823.

[181] M. Cheiky, H. Wilson, Battery separator with fluoride-containing inorganic salt. https://patents.google.com/patent/US6682854, 2001. (Accessed 22 April 2019).

[182] H.In Lee, D.T. Dung, J. Kim, J.H. Pak, S. kyung Kim, H.S. Cho, W.C. Cho, C. H. Kim, The synthesis of a Zirfon-type porous separator with reduced gas crossover for alkaline electrolyzer, Int. J. Energy Res. 44 (2020) 1875–1885, https://doi.org/10.1002/er.5038.

[183] P. Vermeiren, W. Adriansens, J. Moreels, R. Leysen, Evaluation of the ZirfonS separator for use in alkaline water electrolysis and Ni-H2 batteries, Int. J. Hydrogen Energy 23 (1998) 321–324, https://doi.org/10.1016/S0360-3199(97)00069-4.

[184] Palmas Rodríguez, Amores Sánchez-Molina, Campana Mais, Simple and precise approach for determination of ohmic contribution of diaphragms in alkaline water electrolysis, Membranes (Basel) 9 (2019) 129, https://doi.org/10.3390/membranes9100129.

[185] M.B. Amunategui Vallejo, A. Ibanez Llano, M. La, Sierra De Guardia, M. Frades Tapia, D. Gonzalez, in: Rechargeable Zinc-Air Flow Battery, 2014.

[186] D.E. Bergbreiter, K. Kabza, Annealing and reorganization of sulfonated polyethylene films to produce surface-modified films of varying hydrophilicity, J. Am. Chem. Soc. 113 (1991) 1447–1448, https://doi.org/10.1021/ja00004a074.

[187] G.M. Wu, S.J. Lin, C.C. Yang, Preparation and characterization of high ionic conducting alkaline non-woven membranes by sulfonation, J. Membr. Sci. 284 (2006) 120–127, https://doi.org/10.1016/j.memsci.2006.07.025.

[188] J.H. Gordon, S. Balagopal, S. Bhavaraju, J.J. Watkins, Advanced metal-air battery having a ceramic membrane electrolyte. https://patents.google.com/patent/US8012633B2/en, 2007. (Accessed 29 April 2019).

[189] K. Tadanaga, Y. Furukawa, A. Hayashi, M. Tatsumisago, Direct ethanol fuel cell using hydrotalcite clay as a hydroxide ion conductive electrolyte, Adv. Mater. 22 (2010) 4401–4404, https://doi.org/10.1002/adma.201001766.

[190] M.T. Tsehaye, S. Velizarov, B. Van der Bruggen, Stability of polyethersulfone membranes to oxidative agents: a review, Polym. Degrad. Stabil. 157 (2018) 15–33, https://doi.org/10.1016/j.polymdegradstab.2018.09.004.

[191] M.T. Tsehaye, J. Wang, J. Zhu, S. Velizarov, B. Van der Bruggen, Development and characterization of polyethersulfone-based nanofiltration membrane with stability to hydrogen peroxide, J. Membr. Sci. 550 (2018) 462–469, https://doi.org/10.1016/j.memsci.2018.01.022.

[192] A. Le, N. Lieu, S. Pereira, Advanced Polymeric and Organic-Inorganic Membranes for Pressure-Driven Processes Item Type Book Chapter, 2017, https://doi.org/10.1016/B978-0-12-409547-2.12275-9.

[193] N. Wang, Y. Zhao, Coaxial electrospinning, in: Electrospinning Nanofabrication Appl, Elsevier, 2019, pp. 125–200, https://doi.org/10.1016/b978-0-323-51270-1.00005-4.

[194] M.T. Tsehaye, F. Alloin, C. Iojoiu, Prospects for anion-exchange membranes in alkali metal–air batteries, Energies 12 (2019), https://doi.org/10.3390/en12244702.

[195] J. Zhou, P. Zuo, Y. Liu, Z. Yang, T. Xu, Ion exchange membranes from poly(2,6-dimethyl-1,4-phenylene oxide) and related applications, Sci. China Chem. 61 (2018) 1062–1087, https://doi.org/10.1007/s11426-018-9296-6.

[196] H.S. Dang, E.A. Weiber, P. Jannasch, Poly(phenylene oxide) functionalized with quaternary ammonium groups via flexible alkyl spacers for high-performance anion exchange membranes, J. Mater. Chem. A 3 (2015) 5280–5284, https://doi.org/10.1039/c5ta00350d.

[197] Y. He, J. Pan, L. Wu, Y. Zhu, X. Ge, J. Ran, Z.J. Yang, T. Xu, A novel methodology to synthesize highly conductive anion exchange membranes, Sci. Rep. 5 (2015) 1–7, https://doi.org/10.1038/srep13417.

[198] G. Jiang, M. Goledzinowski, F.J.E. Comeau, H. Zarrin, G. Lui, J. Lenos, A. Veileux, G. Liu, J. Zhang, S. Hemmati, J. Qiao, Z. Chen, Free-standing functionalized graphene oxide solid electrolytes in electrochemical gas sensors, Adv. Funct. Mater. 26 (2016) 1729–1736, https://doi.org/10.1002/adfm.201504604.

[199] H.S. Dang, P. Jannasch, Exploring different cationic alkyl side chain designs for enhanced alkaline stability and hydroxide ion conductivity of anion-exchange membranes, Macromolecules 48 (2015) 5742–5751, https://doi.org/10.1021/acs.macromol.5b01302.

[200] N. Sun, F. Lu, A. Mariani, S. Passerini, X. Gao, L. Zheng, Anion exchange membrane electrolyte preserving inverse Ia3¯d bicontinuous cubic phase: effect of microdomain morphology on selective ion transport, J. Membr. Sci. 605 (2020) 118113, https://doi.org/10.1016/j.memsci.2020.118113.

[201] O. Kwon, H.J. Hwang, Y. Ji, O.S. Jeon, J.P. Kim, C. Lee, Y.G. Shul, Transparent bendable secondary zinc-air batteries by controlled void ionic separators, Sci. Rep. 9 (2019) 1–9, https://doi.org/10.1038/s41598-019-38552-4.

[202] K.D. Kreuer, G. Portale, A critical revision of the nano-morphology of proton conducting ionomers and polyelectrolytes for fuel cell applications, Adv. Funct. Mater. 23 (2013) 5390–5397, https://doi.org/10.1002/adfm.201300376.

[203] F.I. Allen, L.R. Comolli, A. Kusoglu, M.A. Modestino, A.M. Minor, A.Z. Weber, Morphology of hydrated as-cast Nafion revealed through cryo electron tomography, ACS Macro Lett. 4 (2015) 1–5, https://doi.org/10.1021/mz500606h.

[204] Z. Yuan, H. Zhang, X. Li, Ion conducting membranes for aqueous flow battery systems, Chem. Commun. 54 (2018) 7570–7588, https://doi.org/10.1039/C8CC03058H.

[205] A. Münchinger, K.D. Kreuer, Selective ion transport through hydrated cation and anion exchange membranes I. The effect of specific interactions, J. Membr. Sci. 592 (2019) 117372, https://doi.org/10.1016/j.memsci.2019.117372.

[206] V.G. Artemov, A.A. Volkov, N.N. Sysoev, A.A. Volkov, Conductivity of aqueous HCl, NaOH and NaCl solutions: is water just a substrate? EPL (Europhysics Lett. 109 (2015) 26002, https://doi.org/10.1209/0295-5075/109/26002.

[207] N. Gupta, H.S. Wroblowa, Rechargeable cells with modified MnO2 cathodes, J. Electrochem. Soc. 135 (1988) 2415–2418, https://doi.org/10.1149/1.2095349.

[208] Y. Li, J. Fu, C. Zhong, T. Wu, Z. Chen, W. Hu, K. Amine, J. Lu, Recent advances in flexible Zinc-based rechargeable batteries, Adv. Energy Mater 9 (2019) 1802605, https://doi.org/10.1002/aenm.201802605.

[209] A. Sumboja, M. Lübke, Y. Wang, T. An, Y. Zong, Z. Liu, All-solid-state, foldable, and rechargeable Zn-air batteries based on manganese oxide grown on graphene-coated carbon cloth air cathode, Adv. Energy Mater 7 (2017) 1700927, https://doi.org/10.1002/aenm.201700927.

[210] M.R. Kraglund, M. Carmo, G. Schiller, S.A. Ansar, D. Aili, E. Christensen, J. O. Jensen, Ion-solvating membranes as a new approach towards high rate alkaline electrolyzers, Energy Environ. Sci. 12 (2019) 3313–3318, https://doi.org/10.1039/c9ee00832b.

[211] D. Lee, H.-W. Kim, J.-M. Kim, K.-H. Kim, S.-Y. Lee, Flexible/rechargeable Zn–air batteries based on multifunctional heteronanomat architecture, ACS Appl. Mater. Interfaces 10 (2018) 22210–22217, https://doi.org/10.1021/acsami.8b05215.

[212] C.C. Yang, S.J. Lin, Preparation of alkaline PVA-based polymer electrolytes for Ni-MH and Zn-air batteries, J. Appl. Electrochem. 33 (2003) 777–784, https://doi.org/10.1023/A:1025514620869.

[213] C.C. Yang, S.J. Lin, G.M. Wu, Study of ionic transport properties of alkaline poly (vinyl) alcohol-based polymer electrolytes, Mater. Chem. Phys. 92 (2005) 251–255, https://doi.org/10.1016/j.matchemphys.2005.01.022.

[214] J. Fu, D.U. Lee, F.M. Hassan, Z. Bai, M.G. Park, Z. Chen, Flexible high-energy polymer-electrolyte-based rechargeable zinc-air batteries, Adv. Mater. 27 (2015) 5617–5622, https://doi.org/10.1002/adma.201502853.

[215] Y. Xu, Y. Zhang, Z. Guo, J. Ren, Y. Wang, H. Peng, Flexible, stretchable, and rechargeable fiber-shaped zinc-air battery based on cross-stacked carbon nanotube sheets, Angew. Chem. Int. Ed. 54 (2015) 15390–15394, https://doi.org/10.1002/anie.201508848.

[216] T.N.T. Tran, H.J. Chung, D.G. Ivey, A study of alkaline gel polymer electrolytes for rechargeable zinc–air batteries, Electrochim. Acta 327 (2019) 135021, https://doi.org/10.1016/j.electacta.2019.135021.
[217] C.-C. Yang, S.-J. Lin, Alkaline composite PEO–PVA–glass-fibre-mat polymer electrolyte for Zn–air battery, J. Power Sources 112 (2002) 497–503, https://doi.org/10.1016/S0378-7753(02)00438-X.
[218] X. Fan, J. Liu, Z. Song, X. Han, Y. Deng, C. Zhong, W. Hu, Porous nanocomposite gel polymer electrolyte with high ionic conductivity and superior electrolyte retention capability for long-cycle-life flexible zinc–air batteries, Nano Energy 56 (2019) 454–462, https://doi.org/10.1016/j.nanoen.2018.11.057.
[219] T.A. Witten, L.M. Sander, Diffusion-limited aggregation, a kinetic critical phenomenon, Phys. Rev. Lett. 47 (1981) 1400–1403, https://doi.org/10.1103/PhysRevLett.47.1400.
[220] G. Garcia, E. Ventosa, W. Schuhmann, Complete prevention of dendrite formation in Zn metal anodes by means of pulsed charging protocols, ACS Appl. Mater. Interfaces 9 (2017) 18691–18698, https://doi.org/10.1021/acsami.7b01705.
[221] Q. Zhang, J. Luan, Y. Tang, X. Ji, H.-Y. Wang, Interfacial design of dendrite-free zinc anodes for aqueous zinc-ion batteries, Angew. Chem. Int. Ed. (2020), https://doi.org/10.1002/anie.202000162.
[222] A. Pei, G. Zheng, F. Shi, Y. Li, Y. Cui, Nanoscale nucleation and growth of electrodeposited lithium metal, Nano Lett. 17 (2017) 1132–1139, https://doi.org/10.1021/acs.nanolett.6b04755.
[223] M. Chamoun, B.J. Hertzberg, T. Gupta, D. Davies, S. Bhadra, B. Van Tassell, C. Erdonmez, D.A. Steingart, Hyper-dendritic nanoporous zinc foam anodes, NPG Asia Mater. 7 (2015), https://doi.org/10.1038/am.2015.32 e178–e178.
[224] J.N. Chazalviel, Electrochemical aspects of the generation of ramified metallic electrodeposits, Phys. Rev. A 42 (1990) 7355–7367, https://doi.org/10.1103/PhysRevA.42.7355.
[225] M. Rosso, T. Gobron, C. Brissot, J.N. Chazalviel, S. Lascaud, Onset of dendritic growth in lithium/polymer cells, J. Power Sources 97–98 (2001) 804–806, https://doi.org/10.1016/S0378-7753(01)00734-0.
[226] C. Monroe, J. Newman, Dendrite growth in lithium/polymer systems, J. Electrochem. Soc. 150 (2003), https://doi.org/10.1149/1.1606686. A1377.
[227] F.C. Porter, Zinc Handbook: Properties, Processing, and Use in Design, CRC Press, 1991, https://doi.org/10.1201/9781482276947.
[228] K. Bass, P.J. Mitchell, G.D. Wilcox, J. Smith, Methods for the reduction of shape change and dendritic growth in zinc-based secondary cells, J. Power Sources 35 (1991) 333–351, https://doi.org/10.1016/0378-7753(91)80117-G.
[229] N.A. Hampson, A.J.S. McNeil, The electrochemistry of porous zinc V. The cycling behaviour of plain and polymer-bonded porous electrodes in koh solutions, J. Power Sources 15 (1985) 261–285, https://doi.org/10.1016/0378-7753(85)80078-1.
[230] J.F. Parker, C.N. Chervin, E.S. Nelson, D.R. Rolison, J.W. Long, Wiring zinc in three dimensions re-writes battery performance - dendrite-free cycling, Energy Environ. Sci. 7 (2014) 1117–1124, https://doi.org/10.1039/c3ee43754j.
[231] B.-S. Lee, S. Cui, X. Xing, H. Liu, X. Yue, V. Petrova, H.-D. Lim, R. Chen, P. Liu, Dendrite suppression membranes for rechargeable zinc batteries, ACS Appl. Mater. Interfaces 10 (2018) 38928–38935, https://doi.org/10.1021/acsami.8b14022.
[232] C. Xie, H. Zhang, W. Xu, W. Wang, X. Li, A long cycle life, self-healing zinc-iodine flow battery with high power density, Angew. Chem. 130 (2018) 11341–11346, https://doi.org/10.1002/ange.201803122.
[233] W. Zhang, Z. Tu, J. Qian, S. Choudhury, L.A. Archer, Y. Lu, Design principles of functional polymer separators for high-energy, metal-based batteries, Small 14 (2018) 1703001, https://doi.org/10.1002/smll.201703001.
[234] X. Yu, A. Manthiram, Electrochemical energy storage with mediator-ion solid electrolytes, Joule 1 (2017) 453–462, https://doi.org/10.1016/j.joule.2017.10.011.
[235] L. Li, A. Manthiram, Long-life, high-voltage acidic Zn-air batteries, Adv. Energy Mater 6 (2016) 1502054, https://doi.org/10.1002/aenm.201502054.
[236] C. Xie, Y. Liu, W. Lu, H. Zhang, X. Li, Highly stable zinc-iodine single flow batteries with super high energy density for stationary energy storage, Energy Environ. Sci. 12 (2019) 1834–1839, https://doi.org/10.1039/c8ee02825g.